

Spring 4-2014

Novel Neuroprotective Function of Apical-Basal Polarity Gene crumbs in Amyloid Beta 42 (A β 42) Mediated Neurodegeneration

Andrew Steffensmeier
University of Dayton

Follow this and additional works at: https://ecommons.udayton.edu/uhp_theses



Part of the [Biology Commons](#)

eCommons Citation

Steffensmeier, Andrew, "Novel Neuroprotective Function of Apical-Basal Polarity Gene crumbs in Amyloid Beta 42 (A β 42) Mediated Neurodegeneration" (2014). *Honors Theses*. 26.
https://ecommons.udayton.edu/uhp_theses/26

This Honors Thesis is brought to you for free and open access by the University Honors Program at eCommons. It has been accepted for inclusion in Honors Theses by an authorized administrator of eCommons. For more information, please contact frice1@udayton.edu, mschlangen1@udayton.edu.

Novel Neuroprotective Function of Apical-Basal Polarity Gene *crumbs* in Amyloid Beta 42 (A β 42) Mediated Neurodegeneration



Honors Thesis

Andrew Steffensmeier

Department: Biology

Advisor: Amit Singh, Ph.D.

April 2014

Novel Neuroprotective Function of Apical-Basal Polarity Gene *crumbs* in Amyloid Beta 42 (A β 42) Mediated Neurodegeneration

Honors Thesis

Andrew Steffensmeier

Department: Biology

Advisor: Amit Singh, Ph.D.

April 2014

Abstract

Alzheimer's disease (AD, OMIM: 104300), a progressive neurodegenerative disorder with no cure to date, is caused by the generation of amyloid-beta-42 (A β 42) aggregates that trigger neuronal cell death by unknown mechanism(s). We have developed a transgenic *Drosophila* eye model where misexpression of human A β 42 results in AD like neuropathology in the neural retina. We have identified an apical-basal polarity gene *crumbs* (*crb*) as a genetic modifier of A β 42-mediated-neuropathology. Misexpression of A β 42 caused upregulation of Crb expression, whereas, downregulation of Crb either by RNAi or null allele approach rescued the A β 42-mediated-neurodegeneration. Co-expression of full length Crb with A β 42 increased severity of A β 42-mediated-neurodegeneration, due to three fold induction of cell death in comparison to the wild type. Higher Crb levels affect axonal targeting from the retina to the brain. The structure function analysis identified intracellular domain of Crb to be required for A β 42-mediated-neurodegeneration. We demonstrate a novel neuroprotective role of Crb in A β 42-mediated-neurodegeneration.

Dedication or Acknowledgements

Authors thank Bloomington Stock Centre, Developmental Studies Hybridoma Bank (DSHB), Sangchul Nam, Pedro Fernandez-Funez, Justin Kumar, and K Cho for fly reagents and members of Singh and Kango-Singh Lab for the comments. AMS is a Berry Summer Research Institute Scholar and a member of the undergraduate Honors Program at UD. AMS wants to thank his awesome family for all the support!



Table of Contents

Abstract	Title Page
Background	1
Materials and Methods	16
Results	20
Discussion	29
References	31
Data Figures with Legends	39
Appendix	
Publication	53

Background

Alzheimer's disease (AD) is a progressive neurodegenerative disorder with no effective cure to date. In 1906, a German physician by the name of Dr. Alois Alzheimer and his colleague, Dr. Emil Kraepelin, followed a case of a 52 year old woman, Frau Auguste D, who exhibited memory loss and difficulty both talking and comprehending what was said to her [1]. "After her death, Dr. Alzheimer examined her brain and discovered unusual plaques and tangles. These are classic identifiers of the disease, which could only be diagnosed post-mortem with an autopsy" [2]. This woman, who they studied and followed for many years, passed away at the age of 52 and became the first patient to be diagnosed with Alzheimer's disease.

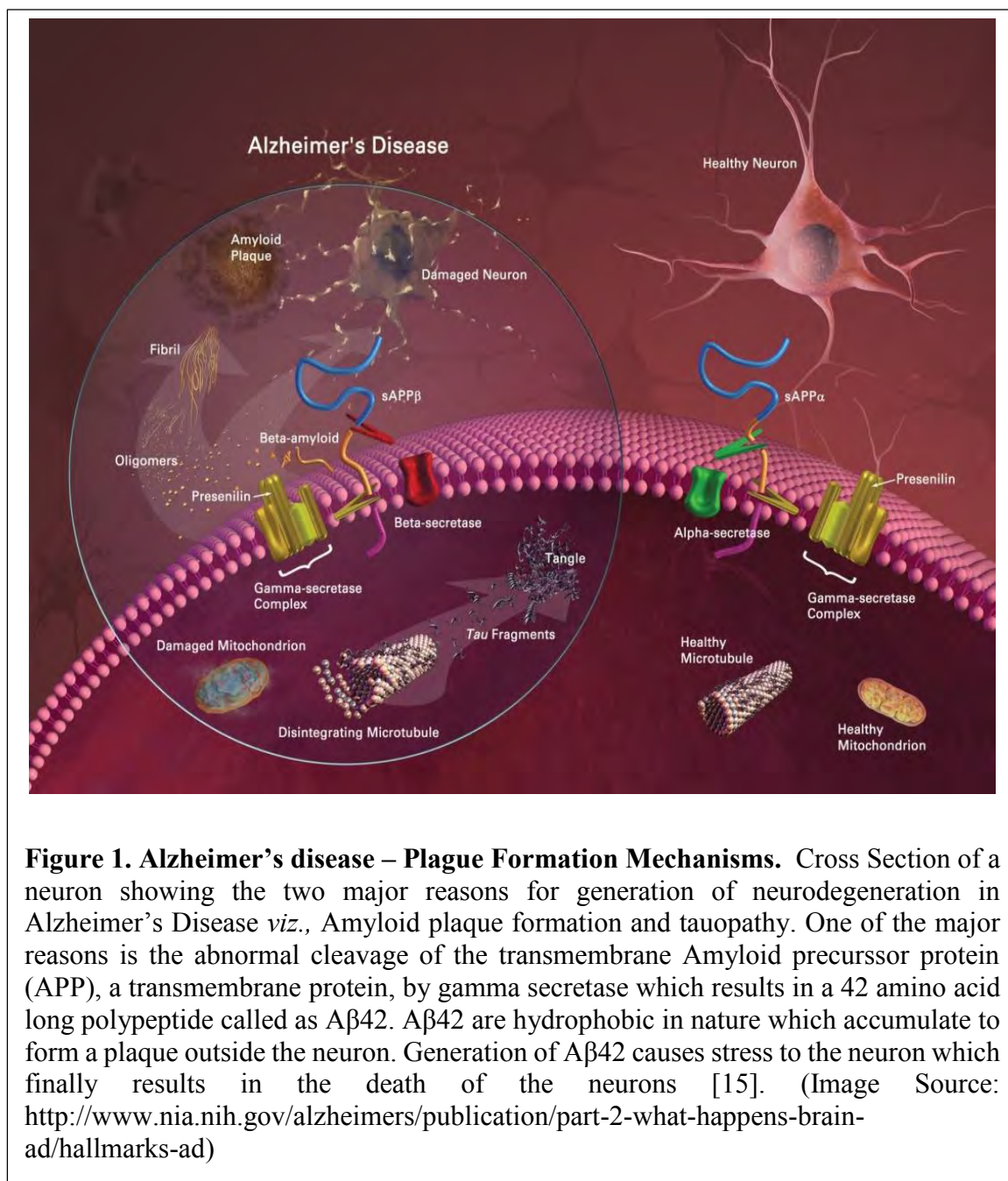
Although it was not until 1906 that the formal name "Alzheimer's" was associated with the disease, there have been many writings about similar symptoms seen in Alzheimer's patients. These writing have been dated back to "Egypt in the ninth century B.C., the Maxims of Ptah Holy describe a form of Alzheimer's. A Roman physician, Claudius Galen, who lived from 130 to 200 A.D., recounts symptoms of age-related forgetfulness in his journals. And in the fourteenth century England, there was even a verbal test to check for forgetfulness" [2]. These writings show that Alzheimer's disease may have been around thousands of years ago, but never received a formal diagnosis until the beginning of the 20th century.

The actual cause of AD is unknown. One of the biological mechanisms responsible for the neuronal death in the human brain of AD patients is known and used for research

on model organisms (animals). The mechanism occurs during cleaving of a protein. The protein, called amyloid- β -40 ($A\beta$ 40), is 40 amino acids long. $A\beta$ 40 is used for daily processes in the nervous system, so neurons can communicate with each other to send signals throughout the body. However, in most AD patients, this protein gets cleaved abnormally (or cut incorrectly). Instead of being 40 amino acids long, the protein is 42 amino acids long ($A\beta$ 42) in patients with AD. This small, two amino acid difference has a detrimental effect on the human nervous system (in this case the brain) [3]. As explained later on, this is exactly the model and cDNA that is used in our *Drosophila melanogaster* model.

AD is characterized by the progressive loss of neurons in the hippocampus and cortex causing decline in cognitive and behavioral functions eventually leading to the death of the patient [4,5]. AD neuropathology is associated with two types of abnormal protein deposition in the human brain *viz.*: (1) neurofibrillary tangles (NFTs) containing hyperphosphorylated forms of a microtubule associated protein Tau, and (2) the accumulation of the amyloid-beta ($A\beta$ 42) peptide [3-10]. $A\beta$ 42 is generated by improper (β - and γ -) cleavage of the transmembrane receptor amyloid precursor protein (APP), as well as by mutations linked to familial AD that affect APP processing [11]. The abnormal cleavage of APP causes the protein to be 42 amino acids long ($A\beta$ 42), whereas, the normal length of the protein is 40 amino acids long ($A\beta$ 40) [4,5,9,10]. The amyloid hypothesis suggests that $A\beta$ 42 forms protofibrils and fibrils. Accumulation of $A\beta$ 42 impairs basic cellular processes due to oxidative stress, misregulation of intracellular calcium, ER stress [12], and aberrant signaling through interaction with several receptors [3,7,8,10], which

results in the death of neurons [9]. The pathway of creation of these cytotoxic amyloid plaques is depicted in Figure 1, where outside the cell membrane the A β 42 plaques are



shown, but within the cell the formation of Tau fragments are evident [13,14]. Therefore, it is important to understand the mechanism underlying A β 42 mediated cell death and neurotoxicity.

The human body cannot handle A β 42. Humans cannot breakdown the miscleaved protein, nor can they use it for other functions in the body. What happens to A β 42 is that it forms hard plaque structures, which are deposits of protein fragments that build up between the neurons in the brain. With these plaques, the neurons can no longer communicate with one another, so they die. The neuronal death is so profound that the brain physically shrivels to about two-thirds the size of a normal human brain [16].

AD is an age-related disease, meaning that it progressively gets worse over time. “In its early stages, memory loss is mild, but with late-stage Alzheimer’s, individuals lose the ability to carry on a conversation and respond to their environment” [15]. Once the A β 42 plaques begin to form, the plaques continue to form at a faster rate, which speeds up the neuronal death in the brain, which, in turn, causes memory loss.

The longer one lives with AD, the more severe the memory loss will be. Alzheimer’s is a type of dementia. “Alzheimer’s is the most common form of dementia, a general term for memory loss and other intellectual abilities serious enough to interfere with daily life. Alzheimer’s disease accounts for 50 to 80 percent of dementia cases” [15]. Through clinical and family experience, AD is recognized by the obvious symptom of short-term memory loss or forgetting basic facts, such as a person’s family or children’s names. The memory loss can be detrimental not only to the patient, but also to their loved ones [17]. “Patients usually die of infection, malnutrition, pneumonia, or heart failure . . .

the duration of the disease can be as short as one year and as long as 25 years with an average of eight to ten years”[18]. The duration of the disease is a major reason why caregivers have such a difficult time coping with and taking care of their patients; it is a long, tiring process to help that always ends in the death of the patient. The last years of the life of an Alzheimer’s patient are also hard to deal with because of the progressive memory loss.

In the last twenty years, the focus on Alzheimer’s disease has increased dramatically. The main reason is that many more people are getting diagnosed with the disease and it is estimated that in 2050, more than 16 million people will be living with the disease [19]. “Every 68 seconds, someone in America develops Alzheimer’s” [19]. The number of people affected by Alzheimer’s is rapidly increasing because it is an age-related disease and people are living longer. As the large cohort of “baby boomers” grows older, an increasing number of people are going to develop the disease. “With the 78 million baby boomers now moving into their later years, the amount affected by Alzheimer’s disease is going to exponentially jump”[1]. These numbers are shocking and the disease devastating, which is why it is important for people to study this disease. The hope is that one day in the near future this disease will not destroy a multitude of people’s lives.

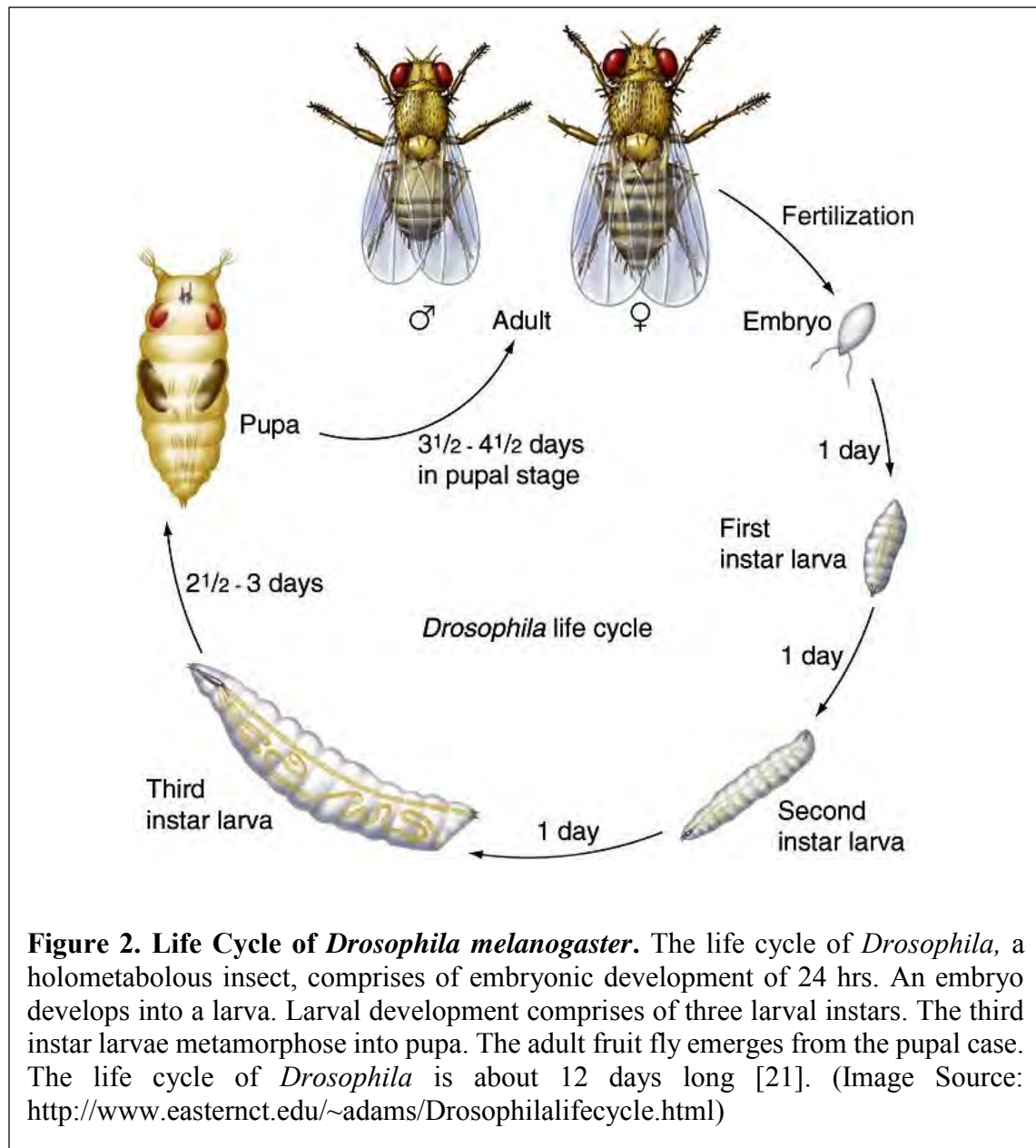
In the United States, money and funding is the main driving force behind research, therapies, and treatment. However, the cost of a particular disease has a nationwide social cost as well as a personal cost for the patient and his or her family. The economic impact of AD is enormous; it totals \$300 billion per year in the United States. Care for one person

with AD is estimated to be \$56,800 a year, the majority of which is paid by the family of the patient with AD [15]. This is an incredible amount of money per patient per year to pay for a disease that will not cure the patient, but will only slow down some of the symptoms. The total economic impact is poised to dramatically increase in the next ten years because the “baby boomers” are now in their sixties. It is important for the costs of caring for these patients to go down as much as possible and for the funding to be amplified now [1].

A group of researchers at Johns Hopkins University in Baltimore, Maryland, have done extensive research into the costs of AD, ways in which the health care system can respond, and how differential responses impact cost. The current situation is summed up in Colantuoni et al.’s (2010) work as they emphasize that projecting the future burden of Alzheimer’s disease is critical for health care planning. They go on to highlight that researchers and policy makers are interested in evaluating the effect of potential interventions that may reduce the risk or slow disease progression [20]. Much of the money going to support the elderly will be going towards care of Alzheimer’s patients, so in essence, money will be saved by investing in Alzheimer’s research now to slow the disease or find a cure. Investments now will result in cost savings later on a national scale.

Since the genetic machinery and basic cell biological pathways are conserved from insects to humans, several animal models have been employed to model AD. Despite the immense amount of information available from modeling AD in animal models such as the mouse [5,9] and the fruit fly [9,22-26], the exact mechanism(s) mediating A β 42-dependent

cell death are yet to be determined. The fruit fly has been a model organism for human diseases for many years since nearly 70% of human disease genes are conserved in flies [27]. In *Drosophila*, the progenitors for all the adult appendages are present as a group of cells set aside in embryo which increase in cell number inside the larva and are called



imaginal disc. Imaginal discs are a favored system for understanding how fields of cells can autonomously regulate growth and pattern formation. Eye imaginal disc arise from 20

cells set aside during embryonic development and develop into the adult eye of *Drosophila* comprising of 9700 cells [28]. We have used a *Drosophila melanogaster* eye model to express the human A β 42 peptide [3]. The *Drosophila melanogaster* eye model has been used to examine other human neurodegenerative diseases, such as Parkinson's disease [9]. There are many reasons the *Drosophila* is used to model neurodegenerative diseases, which include the axonal targeting, neuron structure and functioning, short life cycle, and rather small genome (four chromosomes) that has been completely sequenced [27]. The life cycle of the *Drosophila* is about 12 days from when it is laid as an egg to becoming a reproducing adult and that is shown in Figure 2 below [21].

The *Drosophila* eye model has been extensively employed to investigate patterning, growth, and cell biological processes [9,25-27]. The adult *Drosophila* compound eye develops from an epithelial bi-layer structure housed inside the larva called the eye-antennal imaginal disc, which gives rise to an eye, antenna and head cuticle of the adult fly [29]. A synchronous differentiation event in the developing third instar larval eye imaginal disc differentiates retinal precursor cells to photoreceptor neurons [30]. The eye imaginal disc metamorphose to a pupal retina which develops into the adult eye comprising of about 800 units called ommatidia [30]. Each ommatidium contains eight photoreceptors, pigment cells and several support cells. The eight photoreceptors are made of rhabdomeres, which surround the cone cells. There are four cone cells and two primary pigment cells. The cone cell extends from the cornea of the ommatidium to the cone cell foot at the base, which is where the axon connects to the rhabdomere (R8), which is further shown by Figure 3 of a single ommatidia of the

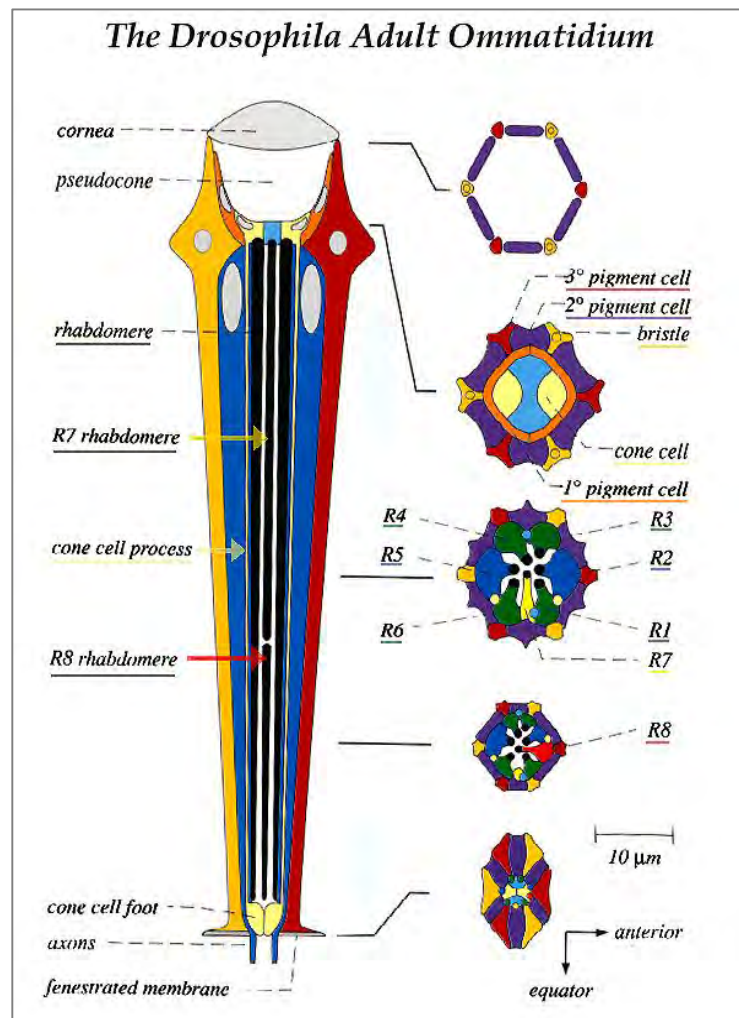


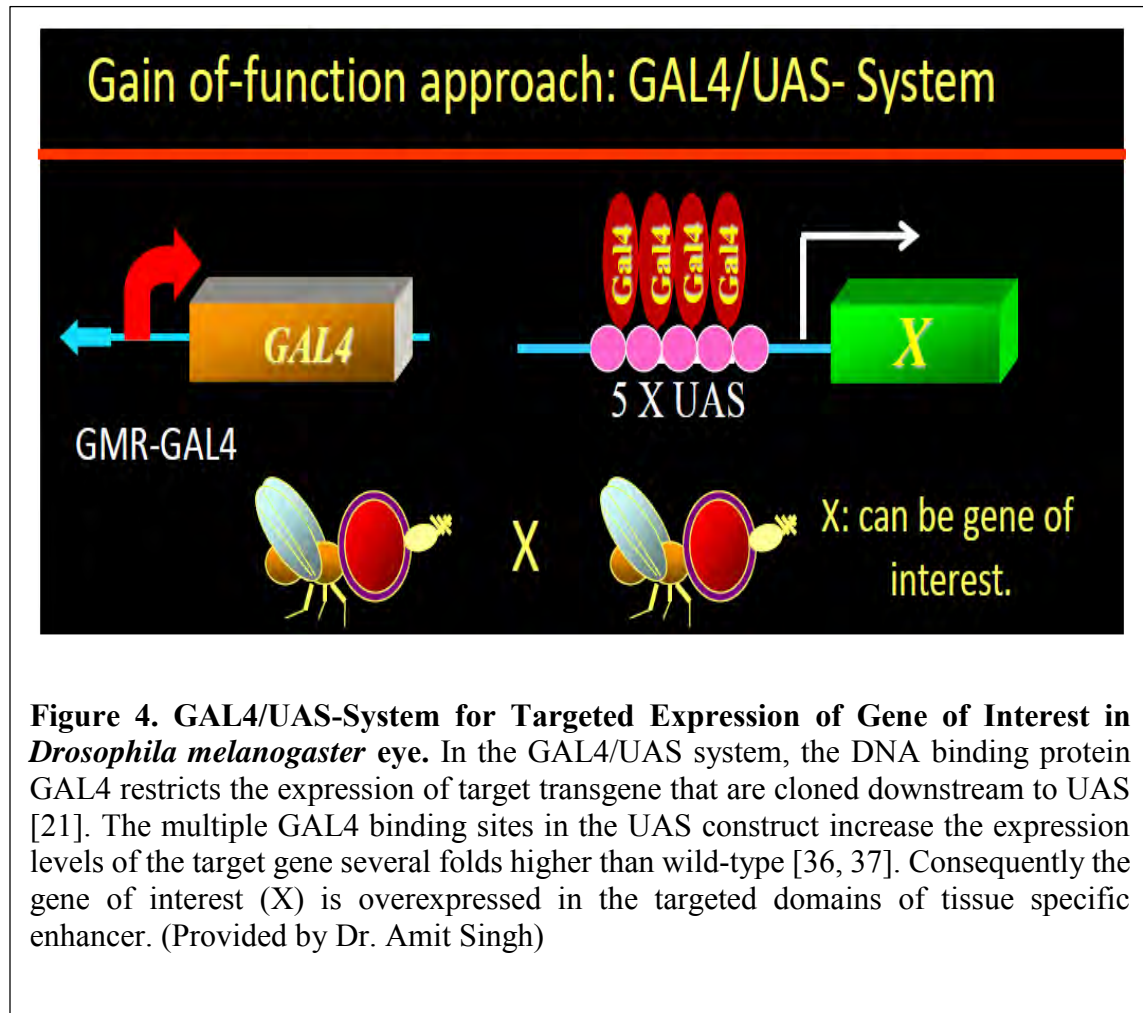
Figure 3. Adult *Drosophila melanogaster* Ommatidium. The adult eye consists of approximately 800 unit eyes or ommatidia. Each ommatidium contains eight photoreceptor cells, each associated with a rhabdomere (a rod-like element containing photoreceptor elements). The photoreceptor cells (1-6) are placed radially around cells 7 and 8, forming an irregular trapezoid. Each ommatidium is surrounded by two primary pigment cells and these are surrounded by six secondary pigment cell shared by neighboring ommatidia. From each ommatidium, eight axons runs posteriorly into a pre-optic stalk and innervate the medulla and lobula of the brain optic lobe [28]. (Donald Ready's Publication)

Drosophila eye [30,31].

In my studies, we examine the effects of A β 42 dependent cell death, which affects the axonal targeting to the photoreceptor neurons (data shown later in figures). The axonal connection is one way to examine the positive or negative effects that a specific gene has on neurodegeneration. In the pupal retina, the extra undifferentiated cells are eliminated by programmed cell death (PCD) [32]. PCD is not observed during earlier stages of larval eye development, however, abnormal extracellular signaling due to inappropriate levels of morphogens may trigger cell death in the developing larval eye imaginal disc [33]. We have found that A β 42 dependent cell death is mediated, in part, through activation of the JNK signaling pathway [3]. However, blocking the JNK signaling pathway does not completely rescue the A β 42-dependent cell death [3]. Therefore, there may be other genetic components that remain to be identified.

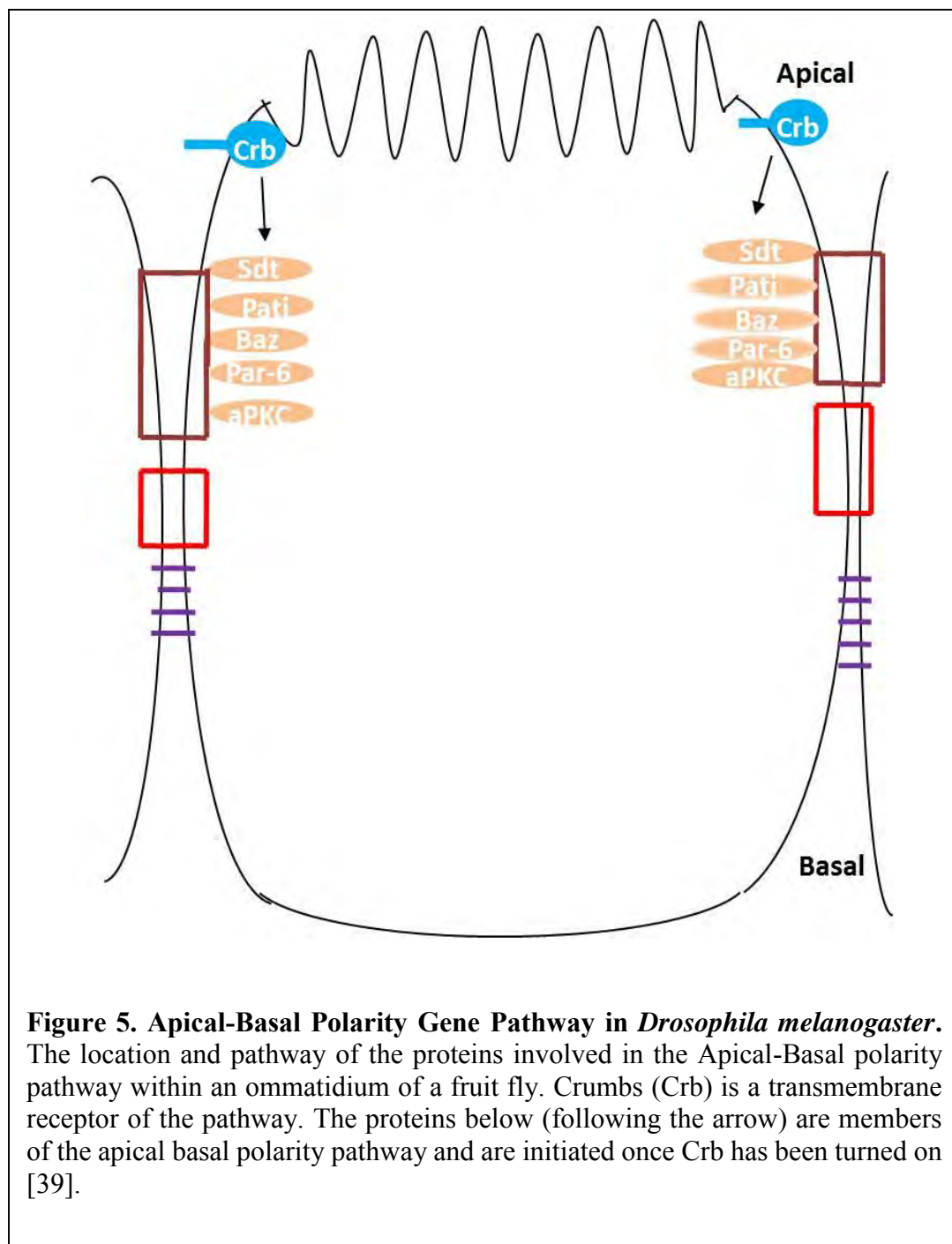
Using the Gal4/UAS system [34], as demonstrated in Figure 4, we have developed an AD model with transgenic flies [3] where high levels of A β 42 are misexpressed in the differentiating photoreceptor neurons of the fly retina using a Glass Multiple Repeat driver [35] (GMR-Gal4>UAS-A β 42, hereafter GMR> A β 42). These GMR> A β 42 transgenic flies exhibit progressive neurodegenerative pathology in the developing retina, which is similar to that observed in AD [3]. Moreover, the misexpression of A β 42 in the differentiating retina (GMR> A β 42) exhibits a stronger neurodegenerative phenotype at 29°C [3]. The AD phenotype that is observed in the *Drosophila* eye can be readily identified, so when a potential modifier, whether genetic or chemical, is present the researcher can determine if there is a significant change via the adult eye structure (size, necrotic spots, color, etc), larvae eye discs, and pupal retina.

The expression of the cell fate marker *disc large* (*dlg*, a membrane specific marker)



was studied in the developing eye imaginal disc. In comparison to the wild type adult eye (Figure 7A) and the larval eye imaginal disc (Figure 7B), misexpression of A β 42 (GMR>A β 42) in the *Drosophila* eye imaginal disc resulted in a reduced eye size with disorganized photoreceptors on the posterior margin as evident from the expression of pan neural marker, Elav (DSHB), in the photoreceptor neurons (Figure 7G), and a highly reduced adult eye which did not show any wild type ommatidium within the compound eye (Figure 7F) [3].

Our earlier studies showed that in the GMR> A β 42 retina, the ommatidia delaminated from the retinal layers possibly due to loss of polarity and/or cell adhesion [3]. We tested various components of the apical-basal polarity gene pathway in a forward gain of function genetic screen by individually co-expressing the apical basal polarity genes with A β 42 (GMR> A β 42 + apical basal polarity genes) in the differentiating photoreceptor neurons. The apical-basal polarity genes involved in this screen included Stardust, Crumbs, APKC, Patj #1 and #2, and various other selected genes. From this screen, we identified a transmembrane protein Crumbs (Crb), as a strong genetic modifier of the A β 42 mediated neurodegenerative phenotype. As a transmembrane protein, Crb, has an extra-cellular domain (ECD), transmembrane domain (TM), which spans the plasma membrane, and then a short intra-cellular domain (ICD), which is key for the AD phenotype relationship that we discovered between Crb and A β 42. Below, Figure 5 shows a cartoon representative of what the Crb protein looks like in the *Drosophila* [38]. Figure 5 shows where the Crb protein is located, which is in the plasma membrane of ommatidia and Crb's order in the apical-basal polarity genes tested [39].



Crb is highly conserved and has three homologs CRB1, CRB2 and CRB3 in humans. An apical basal polarity gene *crb* encodes Crb protein, which is localized to the

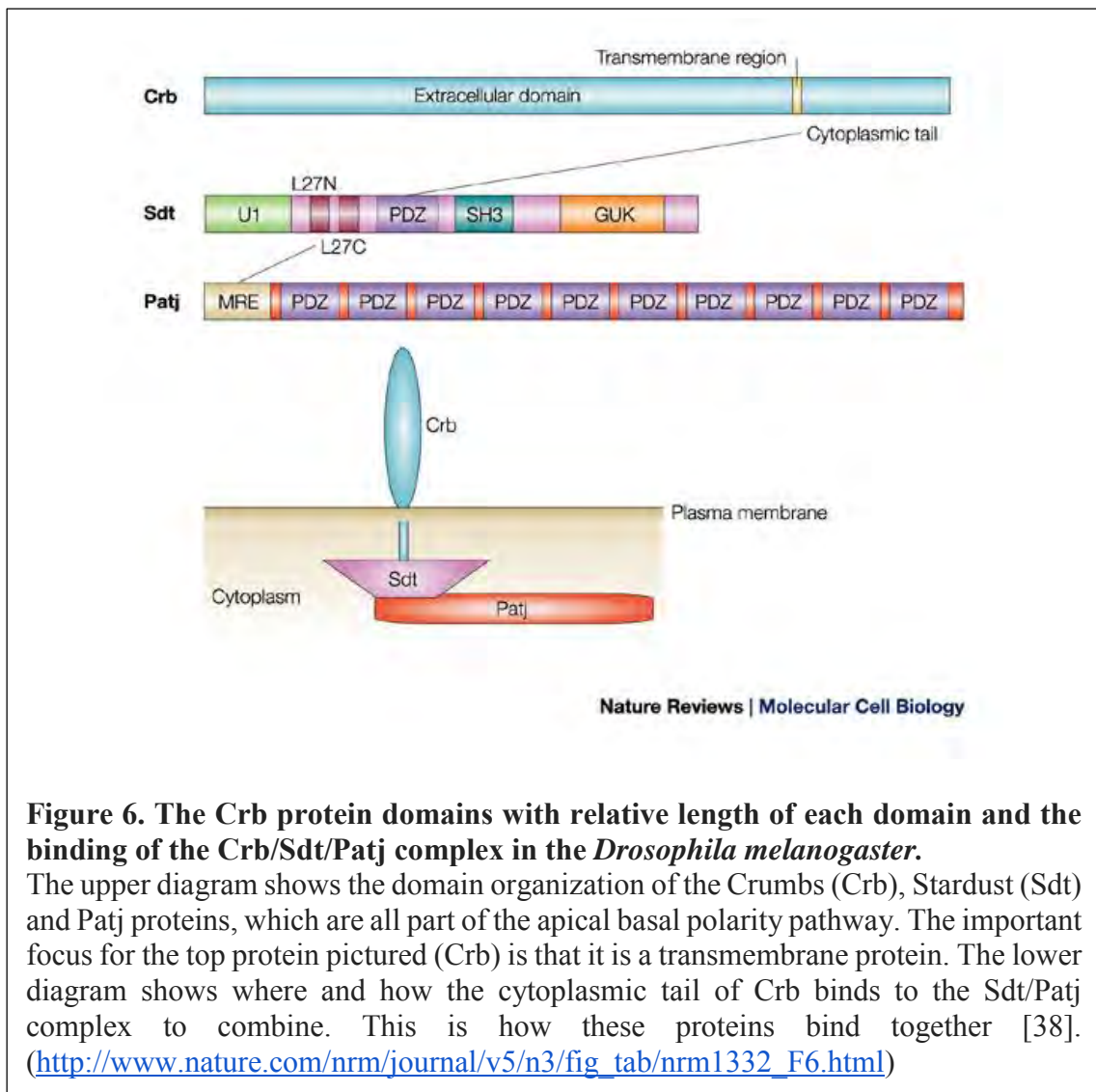


Figure 6. The Crb protein domains with relative length of each domain and the binding of the Crb/Sdt/Patj complex in the *Drosophila melanogaster*.

The upper diagram shows the domain organization of the Crumbs (Crb), Stardust (Sdt) and Patj proteins, which are all part of the apical basal polarity pathway. The important focus for the top protein pictured (Crb) is that it is a transmembrane protein. The lower diagram shows where and how the cytoplasmic tail of Crb binds to the Sdt/Patj complex to combine. This is how these proteins bind together [38]. (http://www.nature.com/nrm/journal/v5/n3/fig_tab/nrm1332_F6.html)

apical domain of the epithelial cells, where it is involved in setting up the apico-basal axis of the cell [40]. Furthermore, Crb is required for organizing apico-basal polarity specification, adherens junctions (AJ) and remodeling in epithelial cells [40,41]. As shown in Figure 6, Crb works by forming a complex with Stardust (Sdt/Pals1) [42]. Sdt, in turn, binds to the intracellular domain of Crb and recruits Pals associated tight junction protein

(Patj) [43] and Lin7 [44]. The pathway described above is depicted in Figure 6 as well as the relative length of the ECD, TM, and ICD of the Crb protein.

CRB1 mutation has been shown to cause vision problems in humans. CRB1 is a genetic disease that is passed as an autosomal recessive mutation that causes blindness and other vision deficiencies. CRB2 in humans is located on chromosome 9 and is found in most of the large tissues of the human (both in the embryo and adult). CRB2 is found in brain, kidney, heart, retina, bladder, etc. CRB3 function is not known because it is such a small protein in humans that not much research has been done or can be done [45]. To date, Crb has not been reported to play any role in A β 42 mediated neurodegeneration in both humans and fruit flies.

Material and Methods

Fly Stocks

All fly stocks used in this study are described in Flybase (<http://flybase.bio.indiana.edu>). The fly stocks used in this study were GMRGal4>UAS-A β 42 (GMR>A β 42) [3], UAS-*crb* Full Length (II), , UAS- *crb*^{intra}, UAS-*crb* myc^{intra}, UAS-*crb*^{intra- Δ PBM}, UAS- *crb* ^{Δ JM}, UAS-myc *crb* ^{Δ JM Δ PBM} [46], V39177, V39178 *crumbs* RNAi (Vienna Drosophila RNAi Center) and FRT82B *crb*^{11A22/TM6B} [40], GMR Gal4 [35].

We have employed Gal4/UAS system for targeted misexpression studies [34]. All Gal4/UAS crosses were maintained at 18°C, 25°C and 29°C, unless specified, to sample different induction levels. The adult fly cultures were maintained at 25°C, while the egg laying (progeny) were transferred to 29°C. Misexpression of A β 42 in the differentiating retina (GMRGal4>UAS-A β 42, GMR> A β 42) exhibits a stronger neurodegenerative phenotype at 29°C [3]. All the targeted misexpression experiments were conducted using the Glass Multiple Repeat driver line (GMR-Gal4), which directs expression of transgenes in the differentiating retinal precursor cells of the developing eye imaginal disc and pupal retina [35].

Immunohistochemistry

Eye-antennal imaginal discs were dissected from third-instar larvae in Phosphate Buffered Saline (PBS) and stained following standard protocol [47]. The protocol involved dissecting the third-instar larvae, fixing the eye-imaginal disc in 16% paraformaldehyde, followed by allowing the eye discs to sit in primary antibody overnight. After primary antibody staining (Table 1), the next step was to stain the eye-imaginal discs using the

secondary antibodies (Table 1) for two hours. The antibodies used are identified in Table 1 by source and concentration. The tissues were then mounted in Vectashield (Vector Laboratories) and immunofluorescent images were captured using the Olympus Fluoview 1000 Confocal Microscope. The final images and figures were prepared using Adobe Photoshop CS4 software.

Table 1. List of the Antibodies Used for Staining Eye-imaginal Discs.

Antibody Used	Prepared in	Concentration Used	Source
Primary Antibodies			
Elav	Rat	1:100	DSHB*
Chaoptin (24B10)	Rat	1:100	DSHB*[48]
Crumbs	Mouse	1:10	DSHB*[40]
Dlg (Discs-large)	Rabbit	1:200	A gift from K. Cho
Secondary Antibodies			
Cy5	Rat	1:200	Jackson Lab
Cy3	Rabbit	1:250	Jackson Lab
Cy3	Mouse	1:200	Jackson Lab
FITC	Rat	1:200	Jackson Lab

*DSHB – Developmental Studies Hybridoma Bank

Crb Staining Protocol

The protocol used for the Crb antibody is different than the protocol used for the other antibodies. A modified protocol was used for Crb staining in the eye imaginal disc [40]. For the Crb staining, once the eye-imaginal discs have been fixed in 16%

paraformaldehyde and washed with PBS after dissection, the discs are washed with 100% acetone twice for ten minutes, then allowed to incubate in the dark in 100% acetone for 20 minutes. After incubation, wash eye-imaginal discs three times with phosphate buffered saline with 0.2% Triton X-100 (PBST). Transfer the tissue to primary antibody diluted in 10% normal donkey serum in phosphate buffered saline with 0.2% Triton X-100 (PBST). Let the sample sit overnight at 4°C. Tissues is washed three times in PBST and then incubated in secondary antibody. It is followed by washed and then tissue is mounted in Vectashield.

Detection of Cell Death

Cell death was detected using TUNEL assays from Roche Diagnostics [49]. TUNEL assays were used to identify the cells undergoing cell death where the cleavage of double and single stranded DNA is labeled by a Fluorescein. The fluorescently labeled nucleotides are added to 3' OH ends in a template-independent manner by Terminal Deoxynucleotidyl transferase (TdT). The fluorescent label tagged fragmented DNA within a dying cell can be detected by fluorescence microscopy. Eye antennal discs after secondary antibody staining [50] were blocked in 10% normal donkey serum in phosphate buffered saline with 0.2% Triton X-100 (PBST) and labeled for TUNEL assays using a cell death detection kit from Roche Diagnostics.

The TUNEL positive cells were counted from five sets of imaginal discs and were used for statistical analysis using Microsoft Excel 2010. The P-values were calculated using one-tailed *t*-test and the error bars represent Standard Deviation from Mean [3].

Adult Eye Imaging

Adult eye images were taken on the Axioimager.Z1 Zeiss Apotome. Adult flies were mounted onto a needle and the image was completed by using extended depth of focus function of the Axiovision software version 4.6.3 by compiling the individual stacks from the Z-sectioning approach. The final images and figures were prepared using Adobe Photoshop CS4 software.

Results

Larval eye imaginal disc (Figure 7B) develops into the adult eye (Figure 7A). Misexpression of A β 42 in the differentiating neurons of the developing eye imaginal disc (GMR> A β 42) results in a strong neurodegenerative phenotype in the adult eye (Figure 7D). We tested Crb protein levels using Crb antibody (Cq4, DSHB) [40] in the GMR> A β 42 eye imaginal disc using a modified protocol [51]. The Crb protein is localized to the apical domain of the epithelial cells. We observed higher levels of Crb protein in the GMR> A β 42 background (Figure 7F) as compared to the wild type eye imaginal disc (Figure 7C). Misexpression of A β 42 peptide with full length Crb [46] using GMR-Gal4 driver (GMR> A β 42+ Crb (FL), as evident from Crb antibody staining (Figure 7I), resulted in increased neurodegeneration as shown by highly disorganized morphology due to clumping of photoreceptor neurons (Red channel, marked by Elav) of neighboring ommatidia of the eye imaginal disc (Figure 7H). Large gaps were observed among the photoreceptors of the ommatidia where the cells begin to die or clump together. The adults failed to form due to early pupal lethality (Figure 7G). These animals died in the early pupal stages; as a result we could not observe any pupal retina like structures (data not shown). Downregulating Crb levels by using a heterozygous combination of FRT82B *crb*^{11A22} allele [52] (Figure 7L) or *crb* RNAi (Figure 7O) resulted in the rescue of the GMR> A β 42 mediated neurodegeneration as seen in the eye imaginal disc (Figure 7K, N) as well as in the adult eye (Figure 7J, M). We found significant rescue although complete restoration to the wild type eye was not seen. These results suggested that higher levels of *crb* are associated with the retina undergoing neurodegeneration due to misexpression of

A β 42. Furthermore, A β 42 mediated neurodegeneration can be rescued by downregulating *crb* function.

We employed TUNEL staining to discern the mechanism of neurodegeneration due to misexpression of Crb in the developing retina. The TUNEL staining marks the nuclei of the dying cells, where the cleavage of double and single stranded DNA is labeled by Fluorescein [49]. Here we utilized TUNEL staining to quantitate the effects of Crb protein levels on neurodegeneration in the GMR> A β 42 background (Figure 8A-F). The TUNEL positive cells were counted from five sets of imaginal discs and were used for statistical analysis using Microsoft Excel 2010. The P-values were calculated using one-tailed *t*-test and the error bars represent Standard Deviation from the Mean [3]. It is known that a few cells undergo cell death in the wild-type eye imaginal disc (Figure 8A) which does not affect the final morphology of the adult compound eye (Figure 7A). The number of TUNEL positive nuclei of the dying cells in the GMR> A β 42 flies (Figure 8B) was almost three times as high when compared to the wild-type eye imaginal disc ($p=1.943 \times 10^{-6}$; Figure 8F). We investigated the levels of Crb with reference to the induction of cell death and found that when Crb levels were increased in a GMR> A β 42 background (GMR> A β 42 +Crb FL), the TUNEL positive cell number increased (Figure 8C) and was almost seven times higher than the wild type eye imaginal disc ($p=9.536 \times 10^{-8}$; Figure 8F) and nearly two times higher than the GMR> A β 42 eye imaginal disc (Figure 8F). Reducing levels of *crb* by using *crb*^{11A22} allele[52] (Figure 8D) or *crb* RNAi (Figure 8E) reduced cell death as evident from reduction in the number of TUNEL positive cells to almost two fold with

respect to the GMR> A β 42 eye imaginal disc (for *crb*^{11A22} p = 8.386x10⁻⁵, for *crb* RNAi p = 8.030x10⁻⁵; Figure 8F).

Next, we investigated the effects of modulating levels of Crb on retinal axon targeting from the retina to the brain using chaoptin (24B10, a marker for photoreceptor cells and their axons [48], DSHB) staining. Disruption of axonal transport mechanisms that leads to axonal vesicle stalling has been shown to contribute to the neurodegenerative phenotypes in the AD fly model [53]. During *Drosophila* visual system development, stereotypical targeting of the axons from the retinal neurons to the special layers of the optic ganglion, medulla and lamina of the brain occurs. The axons of the eight photoreceptor neurons from each ommatidium fasciculate together and project as a single bundle towards the optic lobes of the brain [54]. The *Drosophila* photoreceptors (R cells) seek specific targets to connect in distinct layers of the optic lobes of the brain, viz., R1-R6 axons project to the lamina; R7 and R8 axons project to the separate layers of the medulla[55]. In comparison to the wild-type eye disc where retinal neurons innervate different layers (medulla and lamina) in the brain (Figure 9A), the GMR> A β 42 eye disc shows complete loss of axonal targeting (Figure 9B). Additional upregulation of full length Crb levels in GMR> A β 42 (GMR > A β 42+ Crb FL) strongly affected the retinal axon targeting from the retina to the brain (Figure 9C) as compared to the wild type (Figure 9A) and the GMR> A β 42 alone (Figure 9B). The axonal targeting was restored when *crb* levels were reduced in the GMR> A β 42 background by using either FRT82B *crb*^{11A22} allele (Figure 9D) or *crb* RNAi (Figure 9E). These results further validated our hypothesis that

higher levels of Crb enhanced the neurodegenerative phenotype of A β 42 aggregate accumulation.

In order to discern how different domains of Crb protein (Figure 10A) are involved in preventing GMR> A β 42 mediated neurodegeneration, we used the structure function analysis approach. The full length Crb, a type I transmembrane protein, has 28 EGF domains and four Laminin- AG like repeats in its large extracellular domain (ECD), a transmembrane domain (TM), and a short intracellular domain (ICD) (Figure 10A). The Crb protein's TM domain consists of 37 amino acids spanning the region of the membrane [56]. The ICD contains two motifs, juxtamembrane FERM-binding motif (FBM or JM) domain and C-terminal PDZ (Postsynaptic density/Discs large/ZO-1) binding motif (PBM) domain (Figure 10A). Through its PBM domain, Crb forms a complex with PDZ domain proteins, Stardust and PatJ [42]. It is important to note that the ICD of Crb protein interacts with a variety of conserved proteins including apical basal polarity genes Par6 and aPKC [57, 58]. Prior structure-function studies using the different Crb domains, for example, in the gastrulating embryo, showed that the ubiquitous expression of a membrane-bound cytoplasmic ICD, suppressed the *crb* mutant phenotype to the same extent as full length *crb* [40,46]. Thus, the different domains of Crb carry out different downstream signaling interactions of the protein, so it is important to investigate which domains are involved in the rescue or enhancement of the neurodegeneration caused by A β 42.

We employed targeted misexpression [34] of A β 42 and various domains of Crb protein using the GMR-Gal4 driver [35] for a structure function analysis. The rationale of

these studies was to determine which domain of Crb protein is required for its function in A β 42 mediated neurodegeneration (Figure 7D, E). As discussed previously, in comparison to the wild type eye (Figure 10B), GMR> A β 42 exhibited strong reduction in size due to neurodegeneration as seen in the adult eye (Figure 10C), whereas GMR> Crb [59] resulted in an increase of the adult eye size with minimal necrosis on the margin (Figure 10D)[60]. Targeted misexpression of Crb ICD (the Crb ICD construct used has been referred to as Crb^{intra} [46]; Figure 10A) in a GMR> A β 42 background (GMR> A β 42+ Crb^{intra}) resulted in strong enhancement of the neurodegenerative phenotype of GMR> A β 42 alone as seen in the eye imaginal disc (Figure 10G) as well as in the adult eye (Figure 10F). The GMR> A β 42+ Crb^{intra} adult eye showed strong neurodegeneration as evident from the dark necrotic patch in place of the adult eye (Figure 10F). However, the control GMR> Crb^{intra} also showed some neurodegeneration (Figure 10E), which was not as strong as GMR> A β 42+ Crb^{intra} (Figure 10F). Since both the control (Figure 10E) as well as GMR> A β 42+ Crb^{intra} (Figure 10F, G) showed a neurodegenerative phenotype, it raised the possibility of an additive effect. Further experimentation using the truncated constructs of Crb^{intra} domains disproved this additive effect hypothesis. Targeted misexpression of GMR> A β 42 with Crb^{intra} Δ PBM [46] or Crb^{intra} Δ JM [46] in developing retina resulted in the rescue of the GMR> A β 42 neurodegenerative phenotype as seen in the eye imaginal disc (Figure 10J, M) as well as the adult eye (Figure 10I, L). The controls GMR> Crb^{intra} Δ PBM (Figure 10H) and GMR> Crb^{intra} Δ JM (Figure 10K) exhibit a slightly reduced adult eye. The Crb^{intra} construct lacking both the JM and PBM domains (GMR> Crb^{intra} Δ JM Δ PBM (Figure 10A)) resulted in a near normal adult eye (Figure 10N). Targeted misexpression of GMR> A β 42 with Crb^{intra} Δ JM Δ PBM resulted in the rescue of the GMR> A β 42 neurodegenerative

phenotype as seen in the eye imaginal disc (Fig 10P), and the adult eye (Fig 10O). All these results clearly demonstrated that like the full length Crb (Crb FL), the entire ICD (Crb^{intra}) is also responsible for the enhancement of the neurodegenerative phenotype of GMR> A β 42. It suggests that Crb ICD is sufficient enough to carry out the Crb FL function in A β 42 mediated neurodegeneration. When we remove either one or both of the JM and PBM domains from the ICD of Crb, the GMR> A β 42 phenotype is rescued and the ommatidia are restored to near wild-type. This data strongly indicates that both the JM and PBM domains in Crb are essential to suppress the A β 42 effects. There might be a correlative interaction between the JM and PBM domains of Crb in the A β 42 mediated neurodegeneration. However, when we have an intact ICD or full length Crb, there is a severe enhancement of the GMR> A β 42 phenotype. Also, in the loss-of-function *crb* flies (GMR> A β 42+ *crb*^{11A22} and GMR> A β 42+ *crb* RNAi) where we see reduced Crb level expression (Figure 7L, O) as compared to the wild-type (Figure 7C), there is a rescue of A β 42 mediated neurodegeneration further validating our hypothesis that Crb levels can modify the neurodegenerative phenotype of A β 42 accumulation. Thus, Crb levels can serve as an excellent biomarker for AD.

To further verify the structure function analysis results, TUNEL assays were performed on all of the constructs. The rationale was to examine if the reduced eye phenotype seen in GMR> A β 42+ Crb^{intra} was due to cell death or, on the other hand, if the restored eye as shown by removing either or both of the JM and PBM domains of ICD motifs (Figure 10A) is due to reduced number of TUNEL cells. As mentioned earlier, TUNEL marks the nuclei of dying cells, therefore a reduced number of TUNEL positive

cells nuclei corresponds to less cells dying, which will lead to a rescue of GMR> A β 42 neurodegenerative phenotype in the adult eye. We found that the severely reduced adult eye phenotype of GMR> A β 42+ Crb^{intra} is in fact due to an increase in the number of TUNEL positive cells as compared to the wild-type and the GMR> A β 42 eye disc (Figure 11A, B, I). The GMR> A β 42+ Crb^{intra} exhibits strong neurodegenerative phenotype as evident from disorganized photoreceptor neurons (marked by Elav, green) in the ommatidia. Furthermore, the number of TUNEL positive cells nuclei are increased (Figure 11A, B; red). The TUNEL staining explains the reason for a highly reduced adult eye in GMR> A β 42+ Crb^{intra} (Figure 8F). Additionally, when any either JM or PBM or both JM and PBM domains of the ICD motifs were removed in the GMR> A β 42 background, the severity of neurodegenerative phenotypes was significantly reduced. In GMR> A β 42+ Crb^{intra} Δ JM (Figure 11C, D), GMR> A β 42+ Crb^{intra} Δ PBM (Figure 11E, F), or GMR> A β 42+ Crb^{intra} Δ JM Δ PBM (Figure 11G, H), the number of TUNEL positive dying cells nuclei were significantly less than GMR>A β 42 and GMR> A β 42+ Crb^{intra} (Figure 11I). All of these results further validate the data shown in Figure 4 and conforms to the adult eye phenotypes of each of these structures.

For all the ICD motifs of Crb, the TUNEL positive cells were counted from five sets of imaginal discs and were used for statistical analysis using Microsoft Excel 2010. The P-values were calculated using one-tailed *t*-test and the error bars represent Standard Deviation from the Mean [3]. All the p-values showed the TUNEL count to be significantly different from GMR> A β 42 and the wild-type (Figure 11I). By studying the domains of Crb with reference to the cell death, we found that misexpression of intact Crb ICD domain

in GMR> A β 42 background (GMR> A β 42 +Crb^{intra}), resulted in the increased number of TUNEL positive cell (Figure 11I) and was almost six times higher than the wild type eye imaginal disc ($p=1.5559 \times 10^{-7}$) and nearly two times higher than the GMR> A β 42 eye imaginal disc ($p=8.7869 \times 10^{-8}$). Removing the JM motif alone (GMR> A β 42+ Crb^{intra} Δ JM (Figure 11C, D), PBM motif alone (GMR> A β 42+ Crb^{intra} Δ PBM (Figure 11E, F), or by removing both the ICD motifs (GMR> A β 42+ Crb^{intra} Δ JM Δ PBM (Figure 11G, H) resulted in reduced numbers of TUNEL positive dying cells nuclei. The dying cells nuclei in these truncated constructs (Figure 11C-H) were significantly lower than GMR> A β 42 (for Crb^{intra} Δ JM $p=3.3329 \times 10^{-5}$, for Crb^{intra} Δ PBM $p=1.5028 \times 10^{-5}$, for Crb^{intra} Δ JM Δ PBM $p=8.9278 \times 10^{-6}$; Figure 11I). This TUNEL assay further validated our hypothesis that the reduced eye phenotype seen in GMR> A β 42+ Crb^{intra} (with its fully intact ICD) is primarily due to induction of cell death and the restored eye phenotypes seen when any one or both of the ICD motifs of Crb is/are removed, does indeed have reduced number of dying cells as evident from TUNEL staining.

To further test our hypothesis, we looked at the axonal targeting from the retina to the brain using 24B10 (Chaoptin) in these constructs (Figure 10A). As mentioned earlier, 24B10 shows an organized and orderly axon branching from the retina to the brain in the wild-type background (Figure 9A). However, when we observed the 24B10 staining in the GMR> A β 42+ Crb^{intra} eye there is extreme disorganization marked by the clumping of axons, as well as Elav (red) positive photoreceptors which results in impairing of axonal targeting from retina to the brain (Figure 12A, B). This data further confirms our TUNEL data using GMR> A β 42+ Crb^{intra}. Additionally, when we analyzed other constructs of Crb

by removing either or both of the JM or PBM domains from the ICD motif, there is a rescue of the adult eye (Figure 10A, H-P), a reduction in the number of TUNEL positive (Figure 11C-I), and restoration of the organization of axons from the retina to the brain (Fig 12C-H) in all three constructs (GMR> A β 42+ Crb^{intra Δ JM} (Figure 12C, D), GMR> A β 42+ Crb^{intra Δ PBM} (Figure 12E, F), GMR> A β 42+ Crb^{intra Δ JM Δ PBM} (Figure 12G, H). When the JM motif (GMR> A β 42+ Crb^{intra Δ JM} (Figure 12C, D) or the PBM motif (GMR> A β 42+ Crb^{intra Δ PBM} (Figure 12E, F) was removed, there is restoration of the axonal targeting as evident from the 24B10 staining and marking the axonal projections innervate the two layers of the brain. Furthermore, when we remove both of the ICD motifs (GMR> A β 42+ Crb^{intra Δ JM Δ PBM} (Figure 12G, H), the axonal connection to the brain is restored to near wild type axonal targeting. These data further validates that the ICD domain of Crb is sufficient enough for Crb function in A β 42 mediated neurodegeneration.

Discussion

Our studies strongly suggest that transmembrane protein Crb is involved in A β 42 mediated neurodegeneration. During wing development, N upregulates *crb* transcription at the dorso-ventral (DV) boundary, and the ability of Crb to inhibit the activity of the γ -secretase complex has been proposed to help refine the N activity domain [61]. Crb functions as a negative regulator of the N signaling pathway [60]. Notch is involved in the development and organization of the dorso-ventral boundary through cell proliferation of the developing eye. Because N and Amyloid Precursor Protein (APP) are cleaved by similar secretases [62] and Crb regulates N, the Crb effects on A β 42 could be caused through N regulation. However, in the GMR> A β 42 model used in our studies, the A β 42 protein is already cleaved from APP and does not require cleavage by β - and γ -secretase. Therefore, our data using the transgenic model suggests that Crb also acts downstream of γ -secretase mediated cleavage of APP. Furthermore, higher levels of Crb can enhance human A β 42 mediated neurodegeneration [3]. Thus, Crb role in modulating A β 42 mediated neurodegeneration is downstream of N signaling pathway.

In addition, Crb is an upstream regulator of the organ size growth control pathway *viz.*, Hippo signaling pathway. Recently, it was shown that Crb interacts with its juxtamembrane FERM-binding motif (JM) with the FERM domain of Expanded (Ex) to regulate growth by affecting the Hippo pathway activity [63-65]. Our structure function analysis studies exhibited that ICD of Crb is sufficient for its role in A β 42 mediated

neurodegeneration suggesting that Crb may act independent of its interaction with Hippo pathway member Ex in A β 42 mediated neurodegeneration.

Since Crb ICD is involved in its interaction with apical basal polarity gene localization, there is a strong possibility that higher level of Crb in a GMR> A β 42 background might affect the apical basal polarity of the retinal photoreceptor neurons which result in neurodegeneration. Mutations in Crb homolog 1 (CRB1) has been shown to cause autosomal recessive retinitis pigmentosa (arRP) and autosomal Leber congenital amaurosis (arLCA) [54]. During *Drosophila* eye development, Crb is required in photoreceptors for stalk elongation[60,66], and in preventing light-dependent retinal degeneration [67]. Mutations in the human Crb homolog (CRB1) result in abnormalities like thick retina and lamination problems[45]. Furthermore, mutant Crb protein is thought to be responsible for retinal degenerations[45]. However, in GMR> A β 42 background higher levels of Crb protein were responsible for neurodegeneration. Therefore, it is a strong possibility that higher Crb levels may impair apical basal polarity leading to the A β 42 neurodegeneration. Thus, regulating Crb levels can help prevent the onset of neurodegeneration and Crb may serve as one of the biomarker as well as the key therapeutic targets for the AD.

References:

1. Shriver, Maria, Karen Skelton, Dale Fetherling, and Matt Hickey. *Alzheimer's in America: The Shriver Report on Women and Alzheimer's: A Study*. New York: Simon & Schuster, 2011.
2. Plontz, Michael. "A Brief History of Alzheimer's Disease." *A Brief History of Alzheimer's Disease*. Today's Care Giver, Nov. 2011. Web. June 2012. <http://www.caregiver.com/channels/alz/articles/a_brief_history.htm>.
3. Tare M, Modi RM, Nainaparampil JJ, Puli OR, Bedi S, et al. (2011) Activation of JNK signaling mediates amyloid-ss-dependent cell death. PLoS One 6: e24361.
4. Hardy J (2009) The amyloid hypothesis for Alzheimer's disease: a critical reappraisal. J Neurochem 110: 1129-1134.
5. O'Brien RJ, Wong PC (2010) Amyloid Precursor Protein Processing and Alzheimers Disease. Annu Rev Neurosci.
6. Shankar GM, Li S, Mehta TH, Garcia-Munoz A, Shepardson NE, et al. (2008) Amyloid-beta protein dimers isolated directly from Alzheimer's brains impair synaptic plasticity and memory. Nat Med 14: 837-842.
7. Rincon-Limas DE, Jensen K, Fernandez-Funez P (2012) Drosophila Models of Proteinopathies: the Little Fly that Could. Curr Pharm Des.
8. Pandey UB, Nichols CD (2011) Human disease models in Drosophila melanogaster and the role of the fly in therapeutic drug discovery. Pharmacol Rev 63: 411-436.
9. Hirth F (2010) Drosophila melanogaster in the study of human neurodegeneration. CNS Neurol Disord Drug Targets 9: 504-523.

10. Crews L, Masliah E (2010) Molecular mechanisms of neurodegeneration in Alzheimer's disease. *Hum Mol Genet* 19: R12-20.
11. Finelli A, Kelkar A, Song HJ, Yang H, Konsolaki M (2004) A model for studying Alzheimer's A β 42-induced toxicity in *Drosophila melanogaster*. *Mol Cell Neurosci* 26: 365-375.
12. Casas-Tinto S, Zhang Y, Sanchez-Garcia J, Gomez-Velazquez M, Rincon-Limas DE, et al. (2011) The ER stress factor XBP1s prevents amyloid- β neurotoxicity. *Hum Mol Genet* 20: 2144-2160.
13. U.S. Department of Health and Human Services. *National Plan to Address Alzheimer's Disease*. *Hhs.gov*. 2012b. Web. 20 July 2012. <<http://aspe.hhs.gov/daltcp/napa/NatlPlan.pdf>>.
14. Strooper, Bart De, and James Woodgett. "Alzheimer's Disease: Mental Plaque Removal." *Nature* 423 (2003): 392-93.
15. Alzheimer's Association. "Alzheimer's Disease & Dementia Guide | Alzheimer's Association." *Alzheimer's Disease & Dementia Guide | Alzheimer's Association*. Web. 19 July 2012. <http://www.alz.org/alzheimers_disease_what_is_alzheimers.asp>.
16. Singh A., Chan J., Chern J.J., Choi K.W. 2005. Dorso-ventral Boundary is Required for Organization Growth and Planar Polarity in the *Drosophila* Eye. In *Planar Cell Polarization during Development: Advances in developmental Biology and Biochemistry*. Ed. M. Mlodzik. New York: Elsevier Science and Technology Books: 59-91.

17. Mayo Clinic. "Definition of Alzheimer's Disease." *Mayo Clinic*. Mayo Foundation for Medical Education and Research, 18 Jan. 2011.
18. Wang, Xiao-Ping, and Hong-Liu Ding. "Alzheimer's Disease: Epidemiology, Genetics, and Beyond." *Neuroscience Bulletin* 24.2(2008): 105-9.
19. American Health Assistance Foundation. "A History of Alzheimer's Disease." *A History of Alzheimer's Disease*. 10 Jan. 2012. Web. 30 June 2012. <<http://www.ahaf.org/alzheimers/about/understanding/history.html>>.
20. Colantuoni, Elizabeth, Greg Surplus, Andre Hackman, H. Michael Arrighi, and Ron Brookmeyer. "Web-based Application to Project the Burden of Alzheimer's Disease." *Alzheimer's and Dementia* 6 (2010): 425-28.
21. "Drosophila Melanogaster." *Drosophila Advantages*. Pages 1-2., n.d.
22. Moloney A, Sattelle DB, Lomas DA, Crowther DC (2010) Alzheimer's disease: insights from Drosophila melanogaster models. *Trends Biochem Sci* 35: 228-235.
23. Iijima-Ando K, Iijima K (2010) Transgenic Drosophila models of Alzheimer's disease and tauopathies. *Brain Struct Funct* 214: 245-262.
24. Iijima K, Iijima-Ando K (2008) Drosophila models of Alzheimer's amyloidosis: the challenge of dissecting the complex mechanisms of toxicity of amyloid-beta 42. *J Alzheimers Dis* 15: 523-540.
25. Cowan CM, Shepherd D, Mudher A (2010) Insights from Drosophila models of Alzheimer's disease. *Biochem Soc Trans* 38: 988-992.
26. Cao W, Song HJ, Gangi T, Kelkar A, Antani I, et al. (2008) Identification of novel genes that modify phenotypes induced by Alzheimer's beta-amyloid overexpression in Drosophila. *Genetics* 178: 1457-1471.

27. Bier E (2005) *Drosophila*, the golden bug, emerges as a tool for human genetics. *Nat Rev Genet* 6: 9-23.
28. Wolff, T. and Ready, D. F. (1993). *Pattern formation in the Drosophila retina. In: The Development of Drosophila melanogaster*. Cold Spring Harbor Laboratory Press. Vol. 2 Pp. 1277-1325.
29. Kumar JP (2010) Retinal determination the beginning of eye development. *Curr Top Dev Biol* 93: 1-28.
30. Ready DF, Hanson TE, Benzer S (1976) Development of the *Drosophila* retina, a neurocrystalline lattice. *Dev Biol* 53: 217-240.
31. "Drosophila Melanogaster Ommatidia Structure." *FlyBase.org*. FlyBase, n.d.
32. Brachmann CB, Cagan RL (2003) Patterning the fly eye: the role of apoptosis. *Trends Genet* 19: 91-96.
33. Mehlen P, Mille F, Thibert C (2005) Morphogens and cell survival during development. *J Neurobiol* 64: 357-366.
34. Brand AH, Perrimon N (1993) Targeted gene expression as a means of altering cell fates and generating dominant phenotypes. *Development* 118: 401-415.
35. Moses K, Rubin GM (1991) Glass encodes a site-specific DNA-binding protein that is regulated in response to positional signals in the developing *Drosophila* eye. *Genes Dev* 5: 583-593.
36. Duffy J. (2002). GAL4 system in *Drosophila*: A fly geneticist's swiss army knife. *Genesis*. Vol. 34 Pp. 1-15.
37. Blair S. (2003). Genetic mosaic techniques for studying *Drosophila* development. *Development* 130.40. Tepass U, Theres C, Knust E (1990) crumbs encodes an

- EGF-like protein expressed on apical membranes of *Drosophila* epithelial cells and required for organization of epithelia. *Cell* 61: 787-799.
38. Macara, I (2004). "Parsing the Polarity Code" *Nature Reviews Molecular Cell Biology* 5: 220-31.
39. Verghese S, Waghmare I, Kwon H, Hanes K, Kango-Singh M. (2012). Scribble acts in the *Drosophila* fat-hippo pathway to regulate warts activity. *PLoS One* 7:e47173.10.1371/journal.pone.0047173.
40. Tepass U, Theres C, Knust E (1990) crumbs encodes an EGF-like protein expressed on apical membranes of *Drosophila* epithelial cells and required for organization of epithelia. *Cell* 61: 787-799.
41. Campbell K, Knust E, Skaer H (2009) Crumbs stabilises epithelial polarity during tissue remodelling. *J Cell Sci* 122: 2604-2612.
42. Bachmann A, Schneider M, Theilenberg E, Grawe F, Knust E (2001) *Drosophila* Stardust is a partner of Crumbs in the control of epithelial cell polarity. *Nature* 414: 638-643.
43. Bhat MA, Izaddoost S, Lu Y, Cho KO, Choi KW, et al. (1999) Discs Lost, a novel multi-PDZ domain protein, establishes and maintains epithelial polarity. *Cell* 96: 833-845.
44. Bachmann A, Grawe F, Johnson K, Knust E (2008) *Drosophila* Lin-7 is a component of the Crumbs complex in epithelia and photoreceptor cells and prevents light-induced retinal degeneration. *Eur J Cell Biol* 87: 123-136.

45. Jacobson SG, Cideciyan AV, Aleman TS, Pianta MJ, Sumaroka A, et al. (2003) Crumbs homolog 1 (CRB1) mutations result in a thick human retina with abnormal lamination. *Hum Mol Genet* 12: 1073-1078.
46. Klebes A, Knust E (2000) A conserved motif in Crumbs is required for E-cadherin localisation and zonula adherens formation in *Drosophila*. *Curr Biol* 10: 76-85.
47. Singh A, Kango-Singh M, Sun YH (2002) Eye suppression, a novel function of *teashirt*, requires *Wingless* signaling. *Development* 129: 4271-4280.
48. Zipursky SL, Venkatesh TR, Teplow DB, Benzer S (1984) Neuronal development in the *Drosophila* retina: monoclonal antibodies as molecular probes. *Cell* 36: 15-26.
49. White K, Grether ME, Abrams JM, Young L, Farrell K, et al. (1994) Genetic control of programmed cell death in *Drosophila*. *Science* 264: 677-683.
50. Singh A, Shi X, Choi KW (2006) *Lobe* and *Serrate* are required for cell survival during early eye development in *Drosophila*. *Development* 133: 4771-4781.
51. League GP, Nam SC (2011) Role of kinesin heavy chain in Crumbs localization along the rhabdomere elongation in *Drosophila* photoreceptor. *PLoS One* 6: e21218.
52. Johnson K, Grawe F, Grzeschik N, Knust E (2002) *Drosophila crumbs* is required to inhibit light-induced photoreceptor degeneration. *Curr Biol* 12: 1675-1680.
53. Gunawardena S, Goldstein LS (2001) Disruption of axonal transport and neuronal viability by amyloid precursor protein mutations in *Drosophila*. *Neuron* 32: 389-401.
54. Richard M, Roepman R, Aartsen WM, van Rossum AG, den Hollander AI, et al. (2006) Towards understanding CRUMBS function in retinal dystrophies. *Hum Mol Genet* 15 Spec No 2: R235-243.

55. Garrity PA, Lee CH, Salecker I, Robertson HC, Desai CJ, et al. (1999) Retinal axon target selection in *Drosophila* is regulated by a receptor protein tyrosine phosphatase. *Neuron* 22: 707-717.
56. Laprise P, Beronja S, Silva-Gagliardi NF, Pellikka M, Jensen AM, et al. (2006) The FERM protein Yurt is a negative regulatory component of the Crumbs complex that controls epithelial polarity and apical membrane size. *Dev Cell* 11: 363-374.
57. Nam SC, Choi KW (2003) Interaction of Par-6 and Crumbs complexes is essential for photoreceptor morphogenesis in *Drosophila*. *Development* 130: 4363-4372.
58. Sotillos S, Diaz-Meco MT, Caminero E, Moscat J, Campuzano S (2004) DaPKC-dependent phosphorylation of Crumbs is required for epithelial cell polarity in *Drosophila*. *J Cell Biol* 166: 549-557.
59. Morishima Y, Gotoh Y, Zieg J, Barrett T, Takano H, et al. (2001) Beta-amyloid induces neuronal apoptosis via a mechanism that involves the c-Jun N-terminal kinase pathway and the induction of Fas ligand. *J Neurosci* 21: 7551-7560.
60. Richardson EC, Pichaud F (2010) Crumbs is required to achieve proper organ size control during *Drosophila* head development. *Development* 137: 641-650.
61. Herranz H, Stamatakis E, Feigun F, Milan M (2006) Self-refinement of Notch activity through the transmembrane protein Crumbs: modulation of gamma-secretase activity. *EMBO Rep* 7: 297-302.
62. Kimberly WT, Esler WP, Ye W, Ostaszewski BL, Gao J, et al. (2003) Notch and the amyloid precursor protein are cleaved by similar gamma-secretase(s). *Biochemistry* 42: 137-144.

63. Chen CL, Gajewski KM, Hamaratoglu F, Bossuyt W, Sansores-Garcia L, et al. (2010) The apical-basal cell polarity determinant Crumbs regulates Hippo signaling in *Drosophila*. *Proc Natl Acad Sci U S A* 107: 15810-15815.
64. Ling C, Zheng Y, Yin F, Yu J, Huang J, et al. (2010) The apical transmembrane protein Crumbs functions as a tumor suppressor that regulates Hippo signaling by binding to Expanded. *Proc Natl Acad Sci U S A* 107: 10532-10537.
65. Robinson BS, Huang J, Hong Y, Moberg KH (2010) Crumbs regulates Salvador/Warts/Hippo signaling in *Drosophila* via the FERM-domain protein Expanded. *Curr Biol* 20: 582-590.
66. Richard M, Muschalik N, Grawe F, Ozuyaman S, Knust E (2009) A role for the extracellular domain of Crumbs in morphogenesis of *Drosophila* photoreceptor cells. *Eur J Cell Biol* 88: 765-777.
67. Bulgakova NA, Knust E (2009) The Crumbs complex: from epithelial-cell polarity to retinal degeneration. *J Cell Sci* 122: 2587-2596.
68. Tepass U (1996) Crumbs, a component of the apical membrane, is required for zonula adherens formation in primary epithelia of *Drosophila*. *Dev Biol* 177: 217-225.

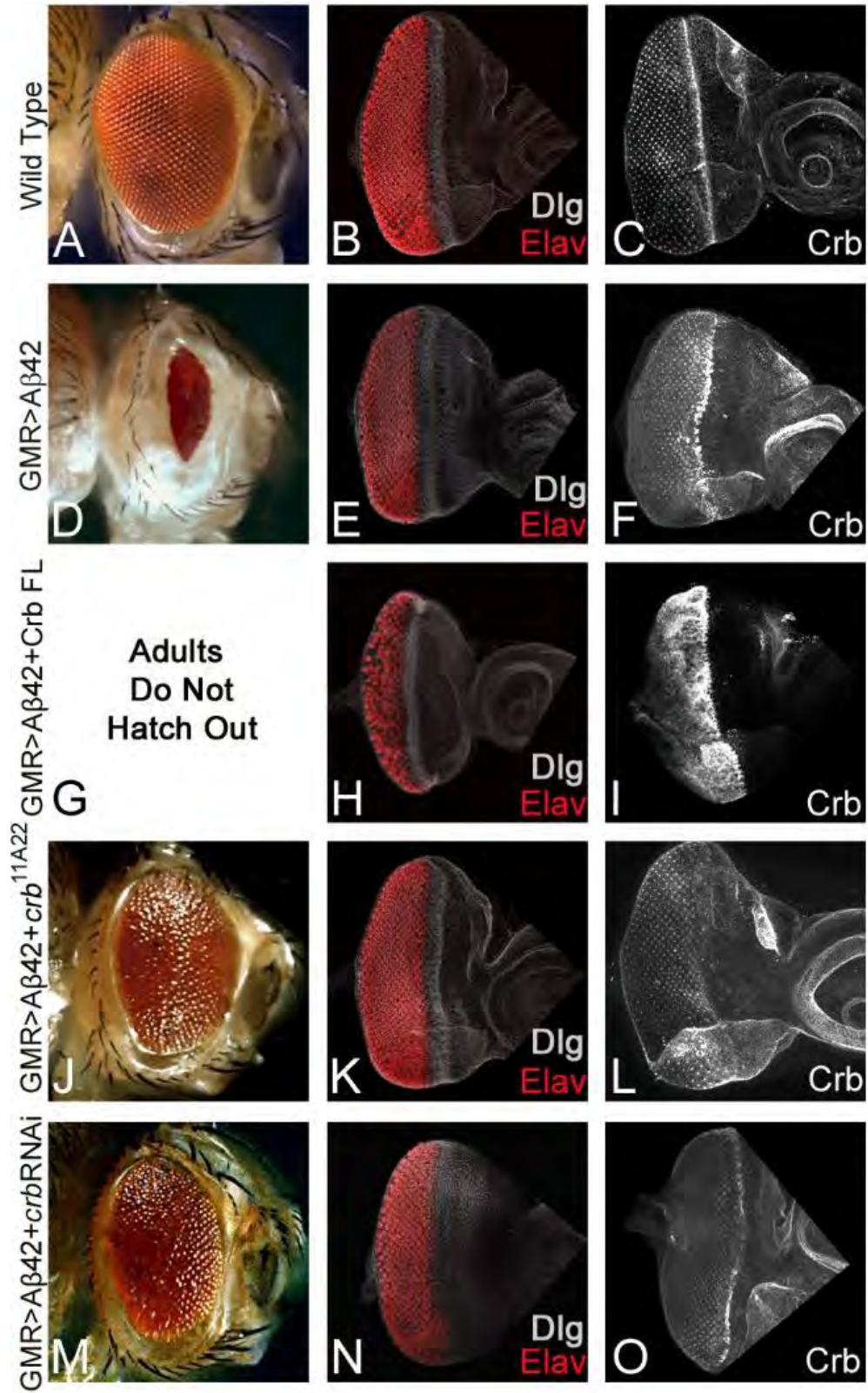
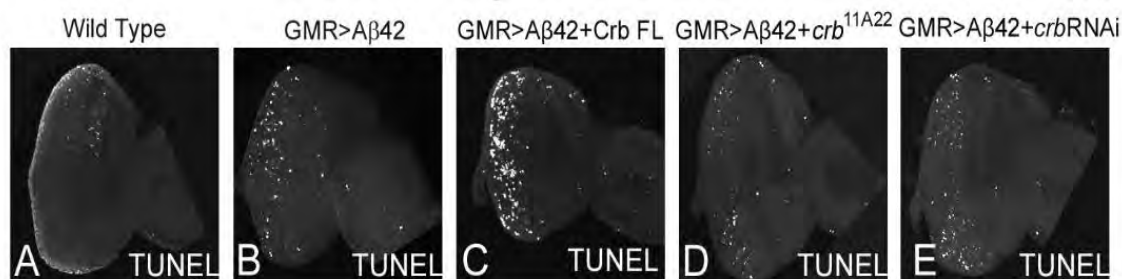


Figure 7. Levels of apical basal polarity gene *crb* modulates A β 42 mediated neurodegeneration. Wild type (A) adult compound eye, a highly organized structure comprising of 750-800 ommatidia[30], which develops from (B, C) eye-imaginal disc. Third-instar eye imaginal disc stained with membrane specific marker, Disc large (Dlg; white), a pan neural marker Elav (red, marks photoreceptors), and (C) Crb protein expression. The Crb expression is localized on the apical surface of epithelial cells and accumulates at the apical membrane's outer margin [68]. (D-F) Misexpression of A β 42 using GMR-Gal4 driver[35] in the differentiating photoreceptor neurons results in the induction of neurodegeneration as seen in (D) the highly reduced adult eye with a glazed surface and (E, F) eye imaginal disc. Note that in GMR> A β 42 eye imaginal discs (E) pan neural marker, Elav, exhibits clumping of the photoreceptor neurons and holes in the developing retina, and (F) strong enrichment of Crb expression in the GMR domain. (G-I) Misexpression of Crb full length [59] in GMR> A β 42 background (GMR> A β 42+ Crb FL) strongly enhances the neurodegeneration phenotype which results in (G) pupal lethality (adults failed to form due to early pupal lethality and as a result lacked the adult eye structure) and (H, I) severe neurodegeneration observed in the eye imaginal disc as evident from (H) fusion of Elav positive photoreceptor neurons, and (I) several fold increase in Crb protein levels. (J-O) Reducing Crb protein levels by using (J-L) *crb*^{11A22} allele [52] (GMR> A β 42+ *crb*^{11A22}) or (M-O) *crb* RNAi (Vienna Drosophila RNAi Center) (GMR> A β 42+ RNAi) result in the significant rescue of GMR> A β 42 mediated neurodegeneration as seen in (J, M) the adult eye and (K, L, N, O) the eye imaginal disc. Note that (L, O) the Crb levels are reduced in these backgrounds.



Cell Death Assay Count

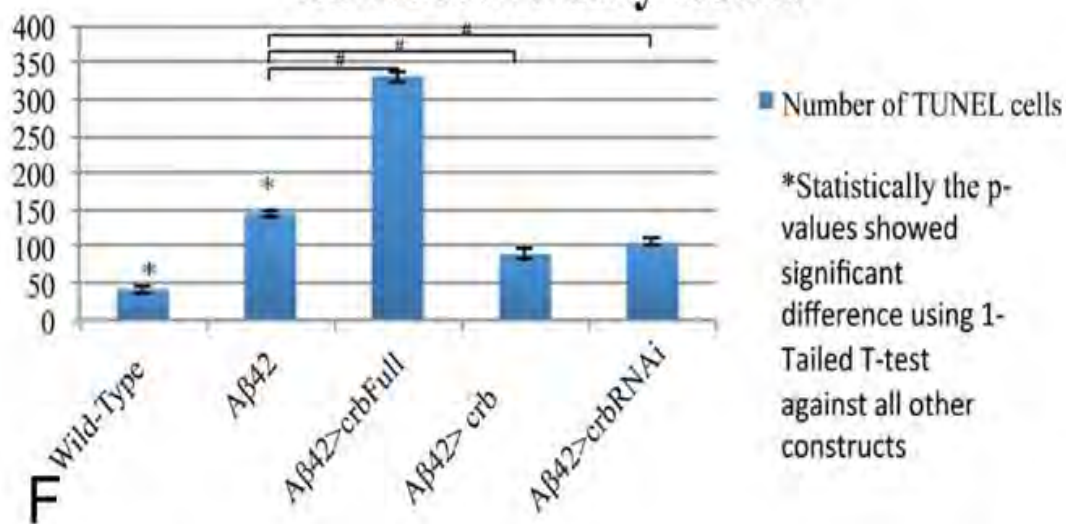


Figure 8. Downregulation of *crb* can block neurodegeneration in the A β 42 background. TUNEL assays are commonly employed to mark the cells undergoing cell death where the cleavage of double and single stranded DNA is labeled by a Fluorescein [49]. (A) Wild type eye imaginal disc showing a few TUNEL positive nuclei. (B) Misexpression of A β 42 using GMR-Gal4 driver[35] in the differentiating photoreceptor neurons results in induction of neurodegeneration (B) as seen by a three-fold induction of cell death as evident from number of TUNEL positive nuclei of the dying cells in comparison to (A) wild type eye imaginal disc. Misexpression of Crb full length (FL) in GMR> A β 42 background (GMR> A β 42+ Crb FL) strongly enhances (C) the neurodegeneration phenotype which results in nearly seven fold increase in number of TUNEL positive nuclei of dying cells in comparison to wild type eye imaginal disc. (D, E) Reducing Crb levels by using (D) *crb*^{11A22} mutant allele [52] (GMR> A β 42+ *crb*^{11A22}) or (E) *crb* RNAi (VDRC) (GMR> A β 42+ RNAi) result in the rescue of GMR> A β 42 mediated neurodegeneration as evident from reduction in numbers of TUNEL positive nuclei of the dying cells. (F) Quantitatively, the number of TUNEL cells have been counted and recorded with all five constructs shown. These phenotypes of enhancement of neurodegenerative phenotype and rescue, based on the number of TUNEL positive cells, are significant as seen by the calculation of P-values based on the one-tailed t-test using Microsoft Excel 2010.

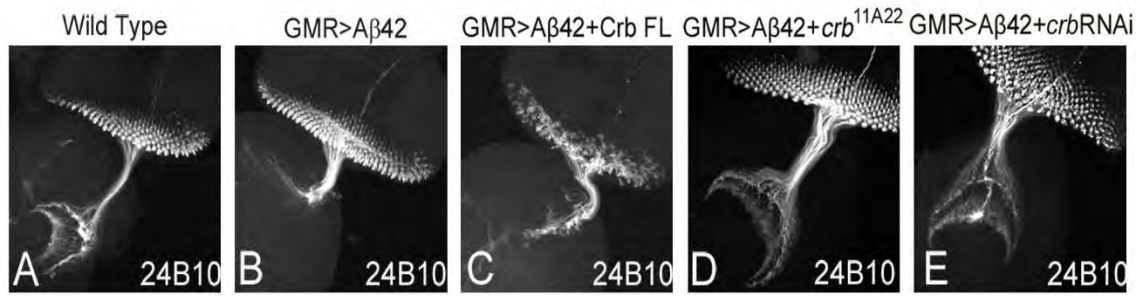


Figure 9. Modulating *crb* levels in the A β 42 background leads to defects in axonal targeting from retina to the brain. (A) Wild Type eye disc stained with sensory neuron marker, Chaoptin (24B10) [48], which marks only photoreceptor neurons and their axons. The photoreceptor neurons extends through the optic stalk and innervate the medulla and lamina of the larval brain. Note that misexpression of A β 42 (GMR> A β 42) in the eye imaginal discs, (B) there is mislocalization of 24B10 expression showing aberrant axonal targeting from retina to brain. The retinal axons fail to innervate the two layers of the brain and end abruptly. (C) Misexpression of Crb full length (FL) in the GMR> A β 42 background (GMR> A β 42+ Crb FL) strongly enhances the neurodegeneration phenotype which results in (C) lack of axonal targeting from retina to brain. Reducing Crb levels by using (D) *crb*^{11A22} allele [52] (GMR> A β 42+ *crb*^{11A22}) or (E) *crb* RNAi (VDRC) (GMR> A β 42+ RNAi) result in the significant rescue of GMR> A β 42 mediated neurodegeneration as evident from the (D, E) restoration of retinal axon targeting.

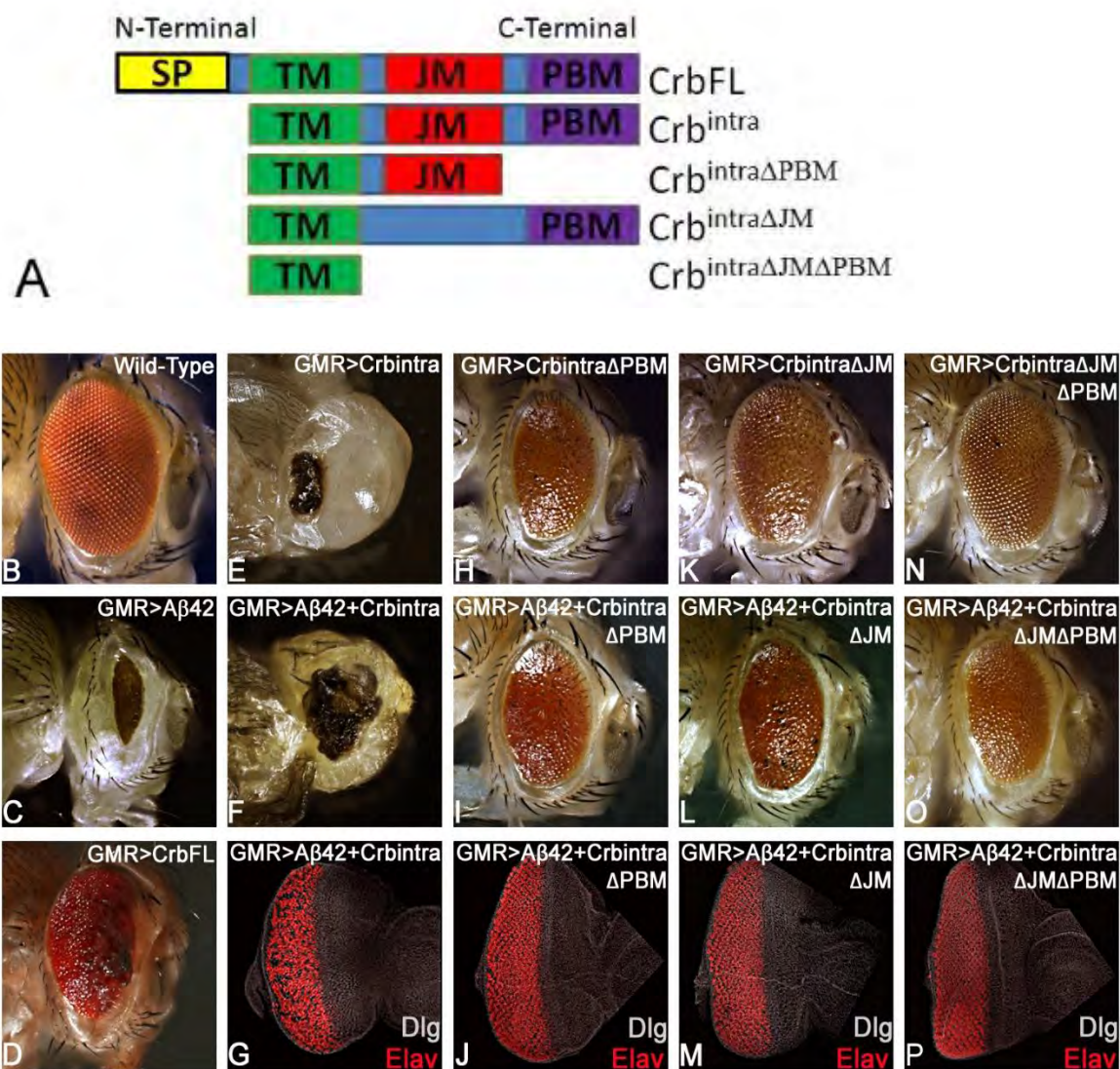


Figure 10. Intracellular domain (ICD) of Crb is required for A β 42 mediated neurodegeneration. (A) A cartoon depicting full length type I transmembrane Crb protein and various truncated constructs used in this study. The full length Crb protein consists of an extracellular domain (ECD), transmembrane domain (TM), and a short cytoplasmic intracellular domain (ICD), which consists of the juxtamembrane Ferm-binding motif (JM) and PDZ-binding motif (PBM) domains [46]. GMR-Gal4 driver was used for the misexpression studies in the differentiating photoreceptor neurons [35]. (B-D) Adult eyes of (B) Wild-Type, (C) GMR> A β 42 (GMR enhancer driving overexpression of human A β 42 in the developing neural retina), and (D) GMR> Crb (FL) are shown as controls. (A, E-F) Misexpression of (E) Crb^{intra} alone, comprising of fully intact ICD, shows a severe phenotype with a small scab on the head cuticle in the adult eye, which is similar to the (F) GMR> A β 42+ Crb^{intra} adult eye. (G) In the GMR> A β 42+ Crb^{intra} eye disc big gaps and holes between photoreceptors of the ommatidia are seen, Dlg (white) marks the membrane and provide an outline of the imaginal disc and pan neural marker Elav marks the photoreceptors. (A, H-P) In the three other Crb constructs, one of the two domains (JM and PBM) of the ICD is either missing or both of them are missing. (H-P) When Crb is missing either (H-J) PBM, or (K-M) JM, or (N-P) both the PBM and JM domain of the ICD, the GMR> A β 42 neurodegenerative phenotype is restored significantly with the adult eye having a larger size, higher number of ommatidia, and interommatidial bristles. Furthermore, the Elav staining in the eye-imaginal discs shows more organized photoreceptors in comparison to the GMR> A β 42 eye imaginal disc. (H, K, N) The controls (H) GMR> Crb^{intra} Δ PBM, (K) GMR> Crb^{intra} Δ JM, and (N) GMR> Crb^{intra} Δ PBM Δ JM showed adult eye phenotypes that are significantly closer to the wild-type. (I, J) When the PBM

domain (GMR> A β 42+ Crb^{intra Δ PBM}) is missing, (I) the adult eye and (J) the eye imaginal disc showed significant rescue in comparison to the GMR> A β 42 phenotype. (L, M) When the JM domain (GMR> A β 42+ Crb^{intra Δ JM}) is missing, (L) the adult eye and (M) the eye-imaginal disc showed significant rescue in comparison to the GMR> A β 42 phenotype. (O, P) Finally, when both PBM and JM domains of the ICD are missing (GMR> A β 42+ Crb^{intra Δ PBM Δ JM}), a significant rescue was seen in (O) the adult eye and (P) the eye imaginal disc in comparison to the GMR> A β 42 phenotype.

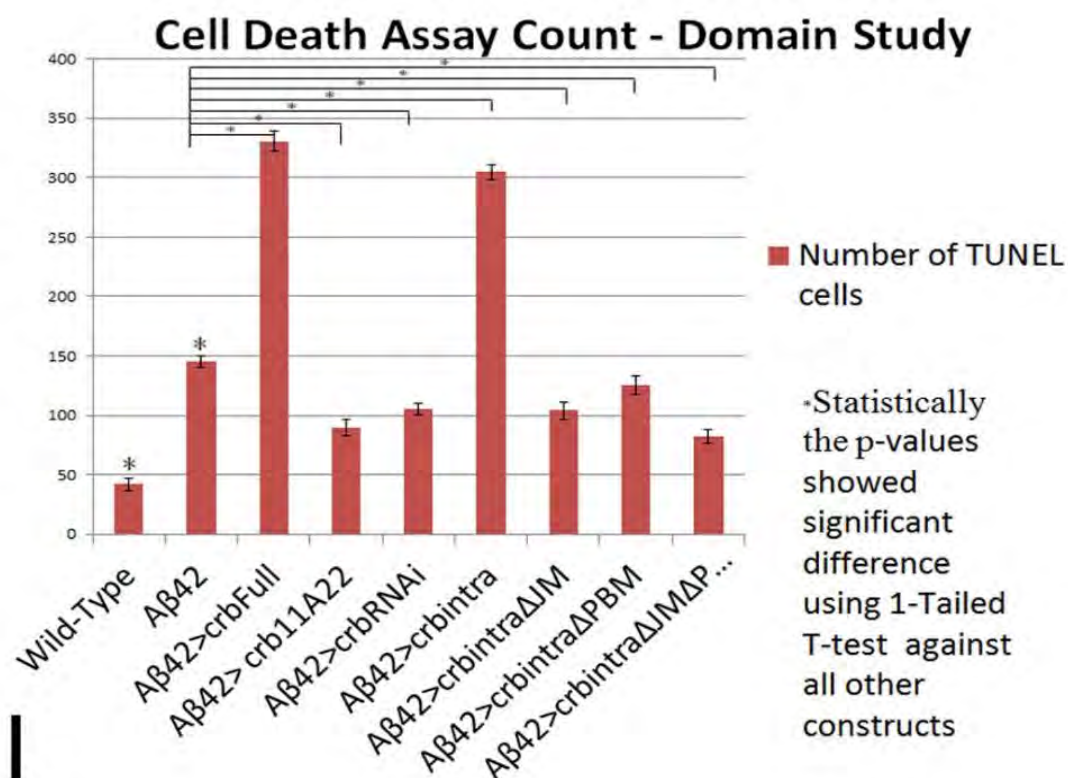
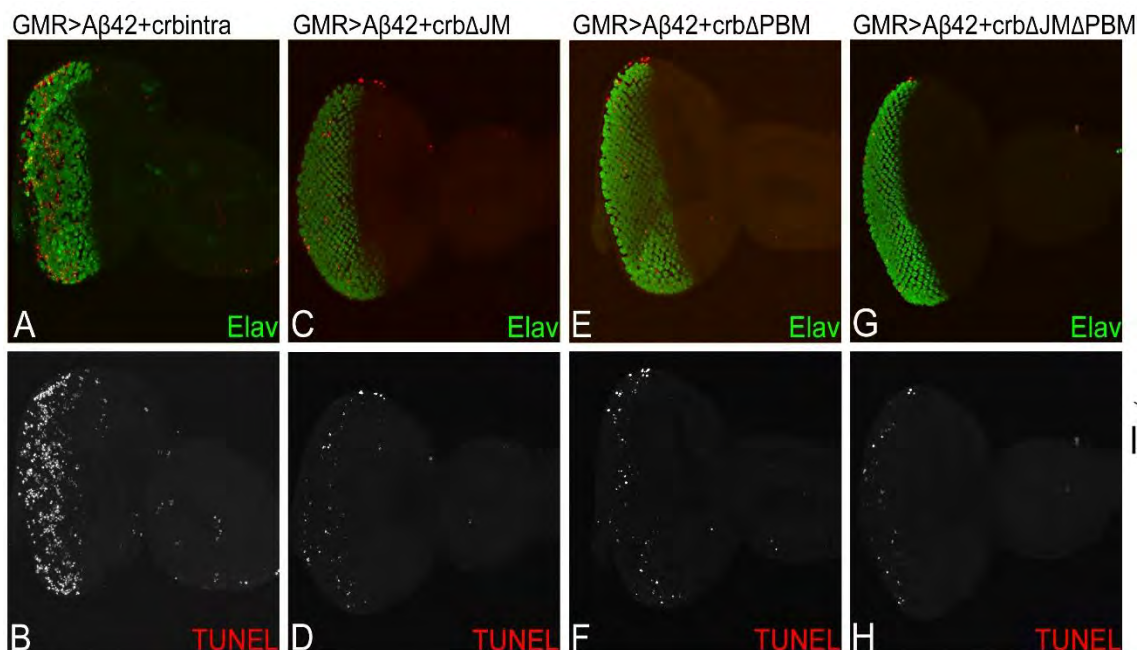


Figure 11. Misexpression of Crb intracellular domain triggers neuronal cell death.

(A, C, E, G) The eye-antennal discs are stained with pan neural marker Elav (green), marking the photoreceptor neurons, and TUNEL (red), which marks the nuclei of dying cells. (B, D, F, H) The split channels of the TUNEL cells are shown for better depiction of the TUNEL cells alone. (A, B) In the $GMR > A\beta 42 + crb^{intra}$ eye disc, the neurodegenerative phenotype of $GMR > A\beta 42$ is enhanced due to increased number of dying photoreceptor neurons as evident from the large number of TUNEL (red) positive cells nuclei, which are (I) calculated quantitatively for all constructs in the bar graph. (A) The dying photoreceptors are clumped and fused together. When we removed either of the PBM, JM or both of these domains within the intracellular domain (ICD) motifs, we see a rescue in the adult eye (Figure 8) and also a (I) decrease in the number of TUNEL positive cells. (C, D) $GMR > A\beta 42 + Crb^{intra} \Delta JM$ (when the JM motif is removed) shows an increase in the (C) organization of the photoreceptors within the ommatidia (Elav) and (C, D, I) a decrease in the number of TUNEL positive cells nuclei as compared to the $GMR > A\beta 42 + Crb^{intra}$. (D) The number of dying cells in $GMR > A\beta 42 + Crb^{intra} \Delta JM$ is closer to that seen in the wild-type. A similar result was found (E, F, I) when PBM domain was removed from the ICD motif, $GMR > A\beta 42 + Crb^{intra} \Delta PBM$ or (G, H, I) when both the JM and PBM domains were removed from the ICD motif $A\beta 42 + Crb^{intra} \Delta JM \Delta PBM$. In comparison to $GMR > A\beta 42 + Crb^{intra}$, we see a significant decrease in the number of TUNEL positive cells in (E, F, I) $GMR > A\beta 42 + Crb^{intra} \Delta PBM$ and (G, H, I), $A\beta 42 + Crb^{intra} \Delta JM \Delta PBM$. (E-H) The number of dying cell nuclei is closer to that seen in the wild-type. Thus, when the ICD is intact (A, B), there is a large number of TUNEL positive cells, which accounts for the adult eye

phenotype observed in Figure 2B. However, when either or both of the ICD motifs are removed (C, D, E, F, G, H), there is a significant reduction in the number of TUNEL positive cells as compared to GMR> A β 42+ Crb^{intra} and GMR>A β 42.

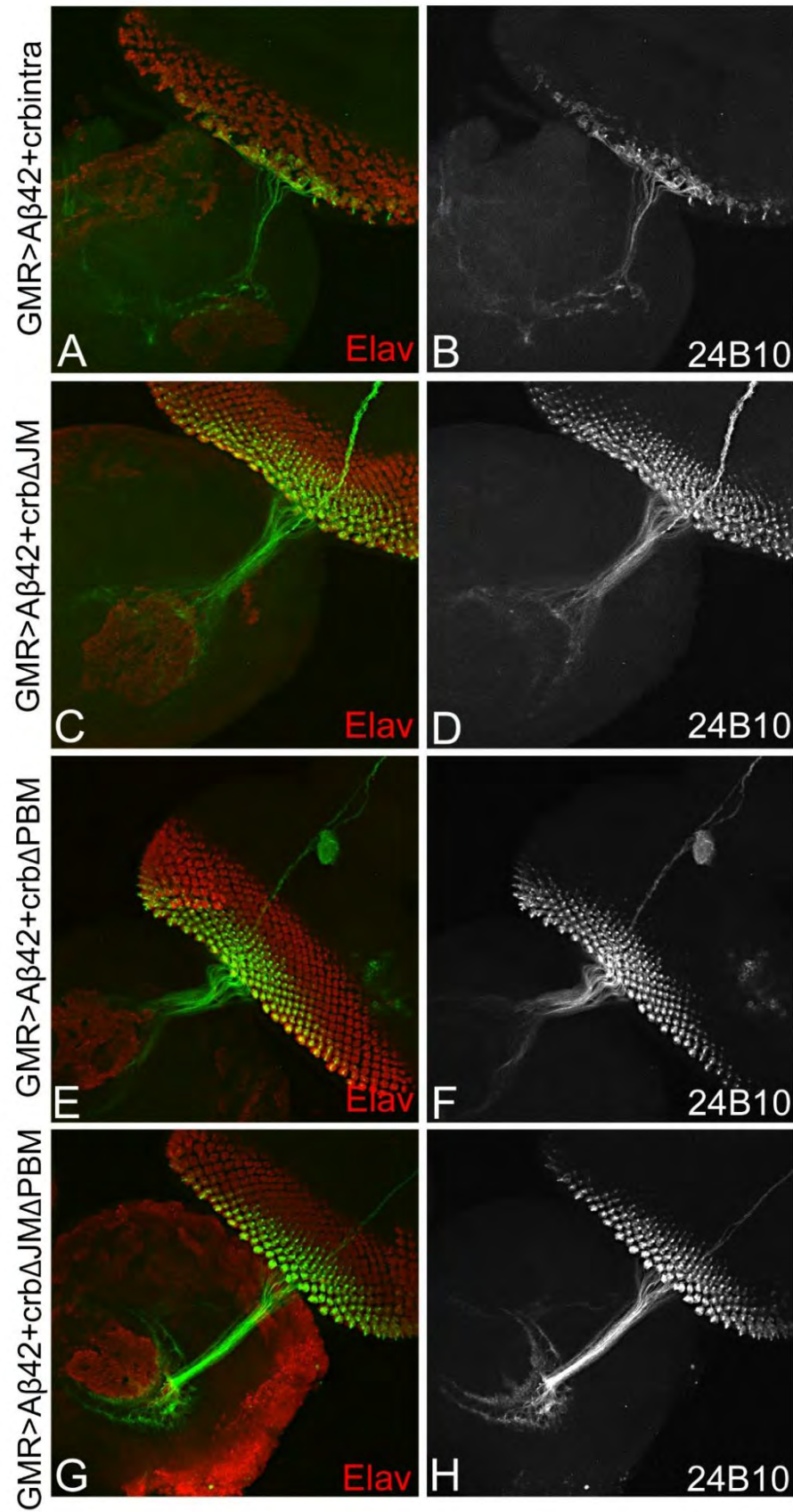


Figure 12. Misexpression of Crb intracellular domain (ICD) can impair axonal targeting. The eye-antennal disc is stained with Elav (red), which marks the photoreceptors, and 24B10 (chaoptin; green), which stains the axons from the retina to the brain [48]. (A, B) Misexpression of intact instar cellular domain ICD $GMR > A\beta 42 + Crb^{intra}$ results in clumping of photoreceptors (Elav; A), disorganization of axonal targeting from the retina to the brain as evident from 24B10 staining. (C, D) When the JM motif using $GMR > A\beta 42 + Crb^{intra \Delta JM}$, photoreceptor organization as well as the axonal targeting is restored to the wild type. Similarly, removing the (E, F) PBM motif of the ICD using $GMR > A\beta 42 + Crb^{intra \Delta PBM}$, or both PBM and JM domain in $GMR > A\beta 42 + Crb^{intra \Delta JM \Delta PBM}$, result in restoration of axonal targeting and photoreceptors. Thus, ICD domain of Crb is required for its role in neurodegeneration.

Appendix:

Novel Neuroprotective Function of Apical-Basal Polarity Gene *Crumbs* in Amyloid Beta 42 (A β 42) Mediated Neurodegeneration

Andrew M. Steffensmeier¹, Meghana Tare², Oorvashi Roy Puli², Rohan Modi¹, Jaison Nainaparampil¹, Madhuri Kango-Singh^{1,2,3*}, Amit Singh^{1,2,3*}

¹ Premedical Program, University of Dayton, Dayton, Ohio, United States of America, ² Department of Biology, University of Dayton, Dayton, Ohio, United States of America, ³ Center for Tissue Regeneration and Engineering at Dayton, University of Dayton, Dayton, Ohio, United States of America

Abstract

Alzheimer's disease (AD, OMIM: 104300), a progressive neurodegenerative disorder with no cure to date, is caused by the generation of amyloid-beta-42 (A β 42) aggregates that trigger neuronal cell death by unknown mechanism(s). We have developed a transgenic *Drosophila* eye model where misexpression of human A β 42 results in AD-like neuropathology in the neural retina. We have identified an apical-basal polarity gene *crumbs* (*crb*) as a genetic modifier of A β 42-mediated-neuropathology. Misexpression of A β 42 caused upregulation of Crb expression, whereas downregulation of Crb either by RNAi or null allele approach rescued the A β 42-mediated-neurodegeneration. Co-expression of full length Crb with A β 42 increased severity of A β 42-mediated-neurodegeneration, due to three fold induction of cell death in comparison to the wild type. Higher Crb levels affect axonal targeting from the retina to the brain. The structure function analysis identified intracellular domain of Crb to be required for A β 42-mediated-neurodegeneration. We demonstrate a novel neuroprotective role of Crb in A β 42-mediated-neurodegeneration.

Citation: Steffensmeier AM, Tare M, Puli OR, Modi R, Nainaparampil J, et al. (2013) Novel Neuroprotective Function of Apical-Basal Polarity Gene *Crumbs* in Amyloid Beta 42 (A β 42) Mediated Neurodegeneration. PLoS ONE 8(11): e78717. doi:10.1371/journal.pone.0078717

Editor: Dhyan Chandra, Roswell Park Cancer Institute, United States of America

Received: August 21, 2013; **Accepted:** September 22, 2013; **Published:** November 18, 2013

Copyright: © 2013 Steffensmeier et al. This is an open-access article distributed under the terms of the Creative Commons Attribution License, which permits unrestricted use, distribution, and reproduction in any medium, provided the original author and source are credited.

Funding: Funding from National Institutes of Health (NIH) grant (1R15 HD064557-01), University of Dayton, Start-up Support. The funders had no role in study design, data collection and analysis, decision to publish, or preparation of the manuscript.

Competing Interests: The authors have declared that no competing interests exist.

* E-mail: asingh1@udayton.edu (AS); mkangosingh1@udayton.edu (MKS)

Background

Alzheimer's disease (AD) is a progressive neurodegenerative disorder with no effective cure to date. AD is characterized by the progressive loss of neurons in the hippocampus and cortex causing decline in cognitive and behavioral functions eventually leading to the death of the patient [1,2]. AD neuropathology is associated with two types of abnormal protein deposition in the human brain viz.: (1) neurofibrillary tangles (NFTs) containing hyperphosphorylated forms of a microtubule associated protein Tau, and (2) the accumulation of the amyloid-beta (A β 42) peptide [1–8]. A β 42 is generated by improper (β - and γ -) cleavage of the transmembrane receptor amyloid precursor protein (APP), as well as by mutations linked to familial AD that affect APP processing [9]. The abnormal cleavage of APP causes the protein to be 42 amino acids long (A β 42), whereas, the normal length of the protein is 40 amino acids long (A β 40) [1,2,7,8]. The amyloid hypothesis suggests that A β 42 forms protofibrils and fibrils. Accumulation of A β 42 impairs basic cellular processes due to oxidative stress, misregulation of intracellular calcium, ER stress [10], and aberrant signaling through interaction with several receptors [3,5,6,8], which results in the death of neurons [7]. Therefore, it is important to understand the mechanism underlying A β 42 mediated cell death and neurotoxicity.

Since the genetic machinery and basic cell biological pathways are conserved from insects to humans, several animal models have

been employed to model AD. Despite the immense amount of information available from modeling AD in animal models such as the mouse [2,7] and the fruit fly [7,11–15], the exact mechanism(s) mediating A β 42-dependent cell death are yet to be determined. The fruit fly has been a model organism for human diseases for many years since nearly 70% of human disease genes are conserved in flies [16]. We have used a *Drosophila melanogaster* eye model to express the human A β 42 peptide [3].

The *Drosophila* eye model has been extensively employed to investigate patterning, growth, and cell biological processes [7,14–16]. The adult *Drosophila* compound eye develops from an epithelial bi-layer structure housed inside the larva called the eye-antennal imaginal disc, which gives rise to an eye, antenna and head cuticle of the adult fly [17]. A synchronous differentiation event in the developing third instar larval eye imaginal disc differentiates retinal precursor cells to photoreceptor neurons [18]. The eye imaginal disc metamorphose to a pupal retina which develops into the adult eye comprising of about 800 units called ommatidia [18]. Each ommatidium contains eight photoreceptors, pigment cells and several support cells. In the pupal retina, the extra undifferentiated cells are eliminated by programmed cell death (PCD) [19]. PCD is not observed during earlier stages of larval eye development, however, abnormal extracellular signaling due to inappropriate levels of morphogens may trigger cell death in the developing larval eye imaginal disc [20]. We have found that A β 42 dependent cell death is mediated, in part, through

activation of the JNK signaling pathway [3]. However, blocking the JNK signaling pathway does not completely rescue the A β 42-dependent cell death [3]. Therefore, there may be other genetic components that remain to be identified.

Using the Gal4/UAS system [21], we have developed an AD model with transgenic flies [3] where high levels of A β 42 are misexpressed in the differentiating photoreceptor neurons of the fly retina using a Glass Multiple Repeat driver [22] (GMR-Gal4>UAS-A β 42, hereafter GMR>A β 42). These GMR>A β 42 transgenic flies exhibit progressive neurodegenerative pathology in the developing retina, which is similar to that observed in AD [3]. Moreover, the misexpression of A β 42 in the differentiating retina (GMR>A β 42) exhibits a stronger neurodegenerative phenotype at 29°C [3]. The expression of the cell fate marker like *disc large* (*dlg*, a membrane specific marker) in the developing eye imaginal disc was studied. In comparison to the wild type adult eye (Figure 1A) and the larval eye imaginal disc (Figure 1B), misexpression of A β 42 (GMR>A β 42) in the *Drosophila* eye imaginal disc resulted in a reduced eye size with disorganized photoreceptors on the posterior margin as evident from the expression of pan neural marker, Elav (DSHB), in the photoreceptor neurons (Figure 1G), and a highly reduced adult eye which did not show any wild type ommatidium within the compound eye (Figure 1F) [3].

Our earlier studies showed that in the GMR>A β 42 retina, the ommatidia delaminated from the retinal layers possibly due to loss of polarity and/or cell adhesion [3]. We tested various components of the apical-basal polarity gene pathway in a forward gain of function genetic screen by individually co-expressing the apical basal polarity genes with A β 42 (GMR>A β 42+apical basal polarity genes) in the differentiating photoreceptor neurons. From this screen, we identified a transmembrane protein Crumbs (Crb), as a strong genetic modifier of the A β 42 mediated neurodegenerative phenotype. Crb is highly conserved and has three homologs CRB1, CRB2 and CRB3 in humans. An apical basal polarity gene *crb* encodes Crb protein, which is localized to the apical domain of the epithelial cells, where it is involved in setting up the apico-basal axis of the cell [23]. Furthermore, Crb is required for organizing apico-basal polarity specification, adherens junctions (AJ) and remodeling in epithelial cells [23,24]. Crb works by forming a complex with Stardust (Sdt/Pals1) [25]. Sdt, in turn, binds to the intracellular domain of Crb and recruits Pals associated tight junction protein (Patj) [26] and Lin7 [27]. To date, Crb has not been reported to play any role in A β 42 mediated neurodegeneration.

Materials and Methods

Fly stocks

All fly stocks used in this study are described in Flybase (<http://flybase.bio.indiana.edu>). The fly stocks used in this study were GMRGal4>UAS-A β 42 (GMR>A β 42) [3], UAS-*crb* Full Length (II), UAS-*crb*^{intra}, UAS-*crb*^{intra Δ PBM}, UAS-*crb*^{intra Δ JM}, UAS-*crb*^{intra Δ JM Δ PBM} [28], V39177, V39178 *crumbs* RNAi (Vienna *Drosophila* RNAi Center) and FRT82B *crb*^{11A22/TM6B} [23], GMR Gal4 [22].

We have employed Gal4/UAS system for targeted misexpression studies [21]. All Gal4/UAS crosses were maintained at 18°C, 25°C and 29°C, unless specified, to sample different induction levels. The adult fly cultures were maintained at 25°C, while the egg laying (progeny) were transferred to 29°C. Misexpression of A β 42 in the differentiating retina (GMRGal4>UAS-A β 42, GMR>A β 42) exhibits a stronger neurodegenerative phenotype at 29°C [3]. All the targeted misexpression experiments were conducted using the Glass Multiple Repeat driver line

(GMR-Gal4), which directs expression of transgenes in the differentiating retinal precursor cells of the developing eye imaginal disc and pupal retina [22].

Immunohistochemistry

Eye-antennal imaginal discs were dissected from third-instar larvae and stained following standard protocol [29]. Antibodies used were rat anti-Elav (1:100), rat anti Chaoptin {24B10 (1:100)}, mouse anti-crumbs (1:10) (Developmental Studies Hybridoma Bank), rabbit anti-Dlg (1:200; a gift from K. Cho). Secondary antibodies (Jackson Laboratory) used were goat anti-rat IgG conjugated with Cy5 (1:200), donkey anti-rabbit IgG conjugated to Cy3 (1:250), donkey anti-mouse IgG conjugated to Cy3 (1:200). The tissues were mounted in Vectashield (Vector Laboratories) and immunofluorescent images were captured using the Olympus Fluoview 1000 Confocal Microscope. A modified protocol was used for Crb staining in the eye imaginal disc [30].

Detection of cell death

Cell death was detected using TUNEL assays from Roche Diagnostics [3,31]. TUNEL assays were used to identify the cells undergoing cell death where the cleavage of double and single stranded DNA is labeled by a Fluorescein. The fluorescently labeled nucleotides are added to 3' OH ends in a template-independent manner by Terminal Deoxynucleotidyl transferase (TdT). The fluorescent label tagged fragmented DNA within a dying cell can be detected by fluorescence microscopy. Eye antennal discs after secondary antibody staining [32] were blocked in 10% normal donkey serum in phosphate buffered saline with 0.2% Triton X-100 (PBT) and labeled for TUNEL assays using a cell death detection kit from Roche Diagnostics.

The TUNEL positive cells were counted from five sets of imaginal discs and were used for statistical analysis using Microsoft Excel 2010. The P-values were calculated using one-tailed *t*-test and the error bars represent Standard Deviation from Mean [3].

Adult eye imaging

Adult eye images were taken on the Axioimager.Z1 Zeiss Apotome. Adult flies were mounted onto a needle and the image was completed by using extended depth of focus function of the Axiovision software version 4.6.3 by compiling the individual stacks from the Z-sectioning approach. The final images and figures were prepared using Adobe Photoshop CS4 software.

Results

We tested Crb protein levels using Crb antibody (Cq4, DSHB) [23] in the GMR>A β 42 eye imaginal disc using a modified protocol [30]. The Crb protein is localized to the apical domain of the epithelial cells. We observed higher levels of Crb protein in the GMR>A β 42 background (Figure 1F) as compared to the wild type eye imaginal disc (Figure 1C). Misexpression of A β 42 peptide with full length Crb [28] using GMR-Gal4 driver (GMR>A β 42+Crb (FL), as evident from Crb antibody staining (Figure 1I), resulted in increased neurodegeneration as shown by highly disorganized morphology due to clumping of photoreceptor neurons (Red channel, marked by Elav) of neighboring ommatidia of the eye imaginal disc (Figure 1H). Large gaps were observed among the photoreceptors of the ommatidia where the cells begin to die or clump together. The adults failed to form due to early pupal lethality (Figure 1G). These animals died in the early pupal stages; as a result we could not observe any pupal retina like structures (data not shown). Downregulating Crb levels by using a heterozygous combination of FRT82B *crb*^{11A22} allele [33]

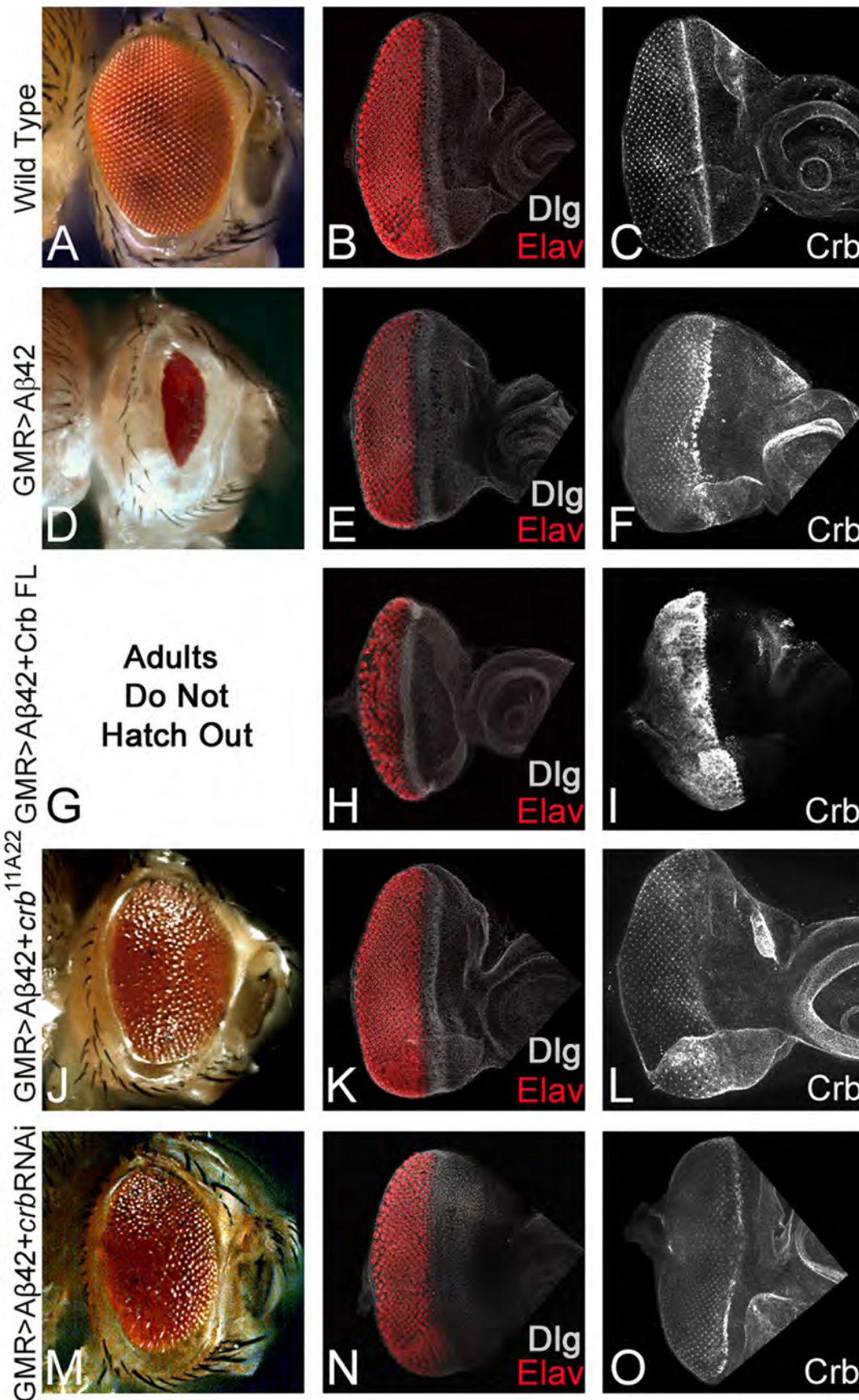


Figure 1. Levels of apical basal polarity gene *crb* modulates A β 42 mediated neurodegeneration. Wild type (A) adult compound eye, a highly organized structure comprising of 750–800 ommatidia [18], which develops from (B, C) eye-imaginal disc. Third-instar eye imaginal disc stained with membrane specific marker, Disc large (Dlg; white), a pan neural marker Elav (red, marks photoreceptors), and (C) Crb protein expression. The Crb expression is localized on the apical surface of epithelial cells and accumulates at the apical membrane's outer margin [51]. (D–F) Misexpression of A β 42 using GMR-Gal4 driver [22] in the differentiating photoreceptor neurons results in the induction of neurodegeneration as seen in (D) the highly reduced adult eye with a glazed surface and (E, F) eye imaginal disc. Note that in GMR>A β 42 eye imaginal discs (E) pan neural marker, Elav, exhibits clumping of the photoreceptor neurons and holes in the developing retina, and (F) strong enrichment of Crb expression in the GMR domain. (G–I) Misexpression of Crb full length [41] in GMR>A β 42 background (GMR>A β 42+Crb FL) strongly enhances the neurodegeneration phenotype which results in (G) pupal lethality (adults failed to form due to early pupal lethality and as a result lacked the adult eye structure) and (H, I) severe neurodegeneration observed in the eye imaginal disc as evident from (H) fusion of Elav positive photoreceptor neurons, and (I) several fold increase in Crb protein levels. (J–O) Reducing Crb protein levels by using (J–L) *crb*^{11A22} allele [33] (GMR>A β 42+*crb*^{11A22}) or (M–O) *crb* RNAi (Vienna Drosophila RNAi Center) (GMR>A β 42+RNAi) result in the significant rescue of GMR>A β 42 mediated neurodegeneration as seen in (J, M) the adult eye and (K, L, N, O) the eye imaginal disc. Note that (L, O) the Crb levels are reduced in these backgrounds.

doi:10.1371/journal.pone.0078717.g001

(Figure 1L) or *crb* RNAi (Figure 1O) resulted in the rescue of the GMR>A β 42 mediated neurodegeneration as seen in the eye imaginal disc (Figure 1K, N) as well as in the adult eye (Figure 1J, M). We found significant rescue although complete restoration to the wild type eye was not seen. These results suggested that higher levels of *crb*s are associated with the retina undergoing neurodegeneration due to misexpression of A β 42. Furthermore, A β 42 mediated neurodegeneration can be rescued by downregulating *crb* function.

We employed TUNEL staining to discern the mechanism of neurodegeneration due to misexpression of Crb in the developing retina. The TUNEL staining marks the nuclei of the dying cells, where the cleavage of double and single stranded DNA is labeled by Fluorescein [31]. Here we utilized TUNEL staining to quantitate the effects of Crb protein levels on neurodegeneration in the GMR>A β 42 background (Figure 2A–F). The TUNEL positive cells were counted from five sets of imaginal discs and were used for statistical analysis using Microsoft Excel 2010. The P-values were calculated using one-tailed *t*-test and the error bars represent Standard Deviation from the Mean [3]. It is known that a few cells undergo cell death in the wild-type eye imaginal disc (Figure 2A) which does not affect the final morphology of the adult compound eye (Figure 1A). The number of TUNEL positive nuclei of the dying cells in the GMR>A β 42 flies (Figure 2B) was almost three times as high when compared to the wild-type eye imaginal disc ($p = 1.943 \times 10^{-6}$; Figure 2F). We investigated the levels of Crb with reference to the induction of cell death and found that when Crb levels were increased in a GMR>A β 42 background (GMR>A β 42+Crb FL), the TUNEL positive cell number increased (Figure 2C) and was almost seven times higher than the wild type eye imaginal disc ($p = 9.536 \times 10^{-8}$; Figure 2F) and nearly two times higher than the GMR>A β 42 eye imaginal disc (Figure 2F). Reducing levels of *crb* by using *crb*^{11A22} allele [33] (Figure 2D) or *crb* RNAi (Figure 2E) reduced cell death as evident from reduction in the number of TUNEL positive cells to almost two fold with respect to the GMR>A β 42 eye imaginal disc (for *crb*^{11A22} $p = 8.386 \times 10^{-3}$, for *crb* RNAi $p = 8.030 \times 10^{-3}$; Figure 2F).

Next, we investigated the effects of modulating levels of Crb on retinal axon targeting from the retina to the brain using chaoptin (24B10, a marker for photoreceptor cells and their axons [34], DSHB) staining. Disruption of axonal transport mechanisms that leads to axonal vesicle stalling has been shown to contribute to the neurodegenerative phenotypes in the AD fly model [35]. During *Drosophila* visual system development, stereotypical targeting of the axons from the retinal neurons to the special layers of the optic ganglion, medulla and lamina of the brain occurs. The axons of the eight photoreceptor neurons from each ommatidium [36] fasciculate together and project as a single bundle towards the optic lobes of the brain. The *Drosophila* photoreceptors (R cells) seek specific targets to connect in distinct layers of the optic lobes

of the brain, *viz.*, R1–R6 axons project to the lamina; R7 and R8 axons project to the separate layers of the medulla [37]. In comparison to the wild-type eye disc where retinal neurons innervate different layers (medulla and lamina) in the brain (Figure 3A), the GMR>A β 42 eye disc shows complete loss of axonal targeting (Figure 3B). Additional upregulation of full length Crb levels in GMR>A β 42 (GMR>A β 42+Crb FL) strongly affected the retinal axon targeting from the retina to the brain (Figure 3C) as compared to the wild type (Figure 3A) and the GMR>A β 42 alone (Figure 3B). The axonal targeting was restored when *crb* levels were reduced in the GMR>A β 42 background by using either FRT82B *crb*^{11A22} allele (Figure 3D) or *crb* RNAi (Figure 3E). These results further validated our hypothesis that higher levels of Crb enhanced the neurodegenerative phenotype of A β 42 aggregate accumulation.

In order to discern how different domains of Crb protein (Figure 4A) are involved in preventing GMR>A β 42 mediated neurodegeneration, we used the structure function analysis approach. The full length Crb, a type I transmembrane protein, has 28 EGF domains and four Laminin- AG like repeats in its large extracellular domain (ECD), a transmembrane domain (TM), and a short intracellular domain (ICD) (Figure 4A). The Crb protein's TM domain consists of 37 amino acids spanning the region of the membrane [38]. The ICD contains two motifs, juxtamembrane FERM-binding motif (FBM or JM) domain and C-terminal PDZ (Postsynaptic density/Discs large/ZO-1) binding motif (PBM) domain (Figure 4A). Through its PBM domain, Crb forms a complex with PDZ domain proteins, Stardust and PatJ [25]. It is important to note that the ICD of Crb protein interacts with a variety of conserved proteins including apical basal polarity genes Par6 and aPKC [39,40]. Prior structure-function studies using the different Crb domains, for example, in the gastrulating embryo, showed that the ubiquitous expression of a membrane-bound cytoplasmic ICD, suppressed the *crb* mutant phenotype to the same extent as full length *crb* [23,28]. Thus, the different domains of Crb carry out different downstream signaling interactions of the protein, so it is important to investigate which domains are involved in the rescue or enhancement of the neurodegeneration caused by A β 42.

We employed targeted misexpression [21] of A β 42 and various domains of Crb protein using the GMR-Gal4 driver [22] for a structure function analysis. The rationale of these studies was to determine which domain of Crb protein is required for its function in A β 42 mediated neurodegeneration (Figure 1D, E). As discussed previously, in comparison to the wild type eye (Figure 4B), GMR>A β 42 exhibited strong reduction in size due to neurodegeneration as seen in the adult eye (Figure 4C), whereas GMR>Crb [41] resulted in an increase of the adult eye size with minimal necrosis on the margin (Figure 4D) [42]. Targeted misexpression of Crb ICD (the Crb ICD construct used has been

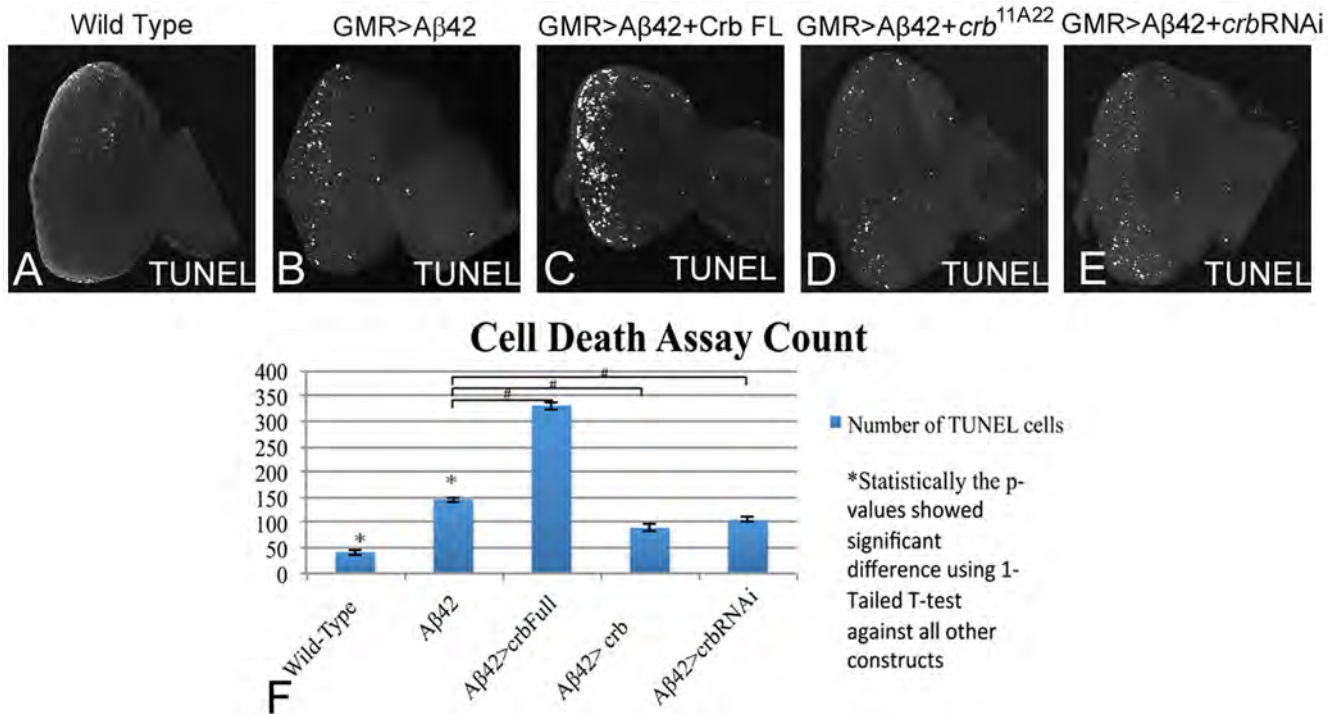


Figure 2. Downregulation of *crb* can block neurodegeneration in the A β 42 background. TUNEL assays are commonly employed to mark the cells undergoing cell death where the cleavage of double and single stranded DNA is labeled by a Fluorescein [31]. (A) Wild type eye imaginal disc showing a few TUNEL positive nuclei. (B) Misexpression of A β 42 using GMR-Gal4 driver [22] in the differentiating photoreceptor neurons results in induction of neurodegeneration (B) as seen by a three-fold induction of cell death as evident from number of TUNEL positive nuclei of the dying cells in comparison to (A) wild type eye imaginal disc. Misexpression of Crb full length (FL) in GMR>A β 42 background (GMR>A β 42+Crb FL) strongly enhances (C) the neurodegeneration phenotype which results in nearly seven fold increase in number of TUNEL positive nuclei of dying cells in comparison to wild type eye imaginal disc. (D, E) Reducing Crb levels by using (D) *crb*^{11A22} mutant allele [33] (GMR>A β 42+*crb*^{11A22}) or (E) *crb* RNAi (VDRC) (GMR>A β 42+RNAi) result in the rescue of GMR>A β 42 mediated neurodegeneration as evident from reduction in numbers of TUNEL positive nuclei of the dying cells. (F) Quantitatively, the number of TUNEL cells have been counted and recorded with all five constructs shown. These phenotypes of enhancement of neurodegenerative phenotype and rescue, based on the number of TUNEL positive cells, are significant as seen by the calculation of P-values based on the one-tailed t-test using Microsoft Excel 2010.
doi:10.1371/journal.pone.0078717.g002

referred to as Crb^{intra} [28]; Figure 4A) in a GMR>A β 42 background (GMR>A β 42+Crb^{intra}) resulted in strong enhancement of the neurodegenerative phenotype of GMR>A β 42 alone as seen in the eye imaginal disc (Figure 4G) as well as in the adult eye (Figure 4F). The GMR>A β 42+Crb^{intra} adult eye showed

strong neurodegeneration as evident from the dark necrotic patch in place of the adult eye (Figure 4F). However, the control GMR>Crb^{intra} also showed some neurodegeneration (Figure 4E), which was not as strong as GMR>A β 42+Crb^{intra} (Figure 4F). Since both the control (Figure 4E) as well as GMR>A β 42+

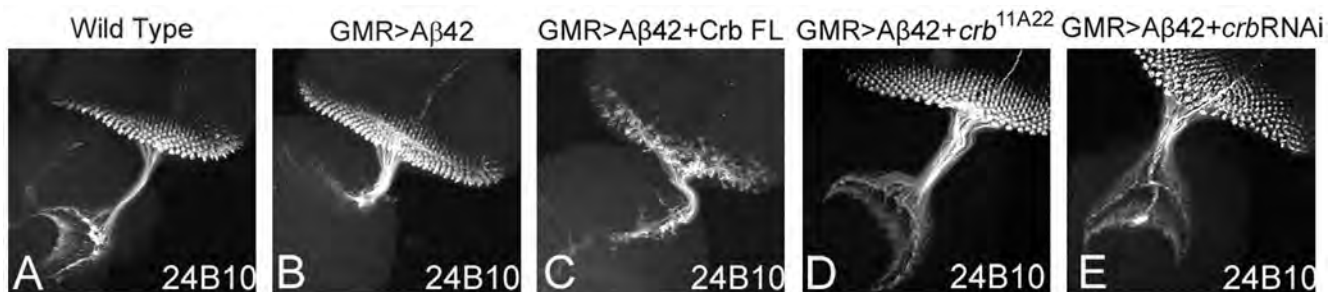


Figure 3. Modulating *crb* levels in the A β 42 background leads to defects in axonal targeting from retina to the brain. (A) Wild Type eye disc stained with sensory neuron marker, Chaoptin (24B10) [34], which marks only photoreceptor neurons and their axons. The photoreceptor neurons extends through the optic stalk and innervate the medulla and lamina of the larval brain. Note that misexpression of A β 42 (GMR>A β 42) in the eye imaginal discs, (B) there is mislocalization of 24B10 expression showing aberrant axonal targeting from retina to brain. The retinal axons fail to innervate the two layers of the brain and end abruptly. (C) Misexpression of Crb full length (FL) in the GMR>A β 42 background (GMR>A β 42+Crb FL) strongly enhances the neurodegeneration phenotype which results in (C) lack of axonal targeting from retina to brain. Reducing Crb levels by using (D) *crb*^{11A22} allele [33] (GMR>A β 42+*crb*^{11A22}) or (E) *crb* RNAi (VDRC) (GMR>A β 42+RNAi) result in the significant rescue of GMR>A β 42 mediated neurodegeneration as evident from the (D, E) restoration of retinal axon targeting.
doi:10.1371/journal.pone.0078717.g003

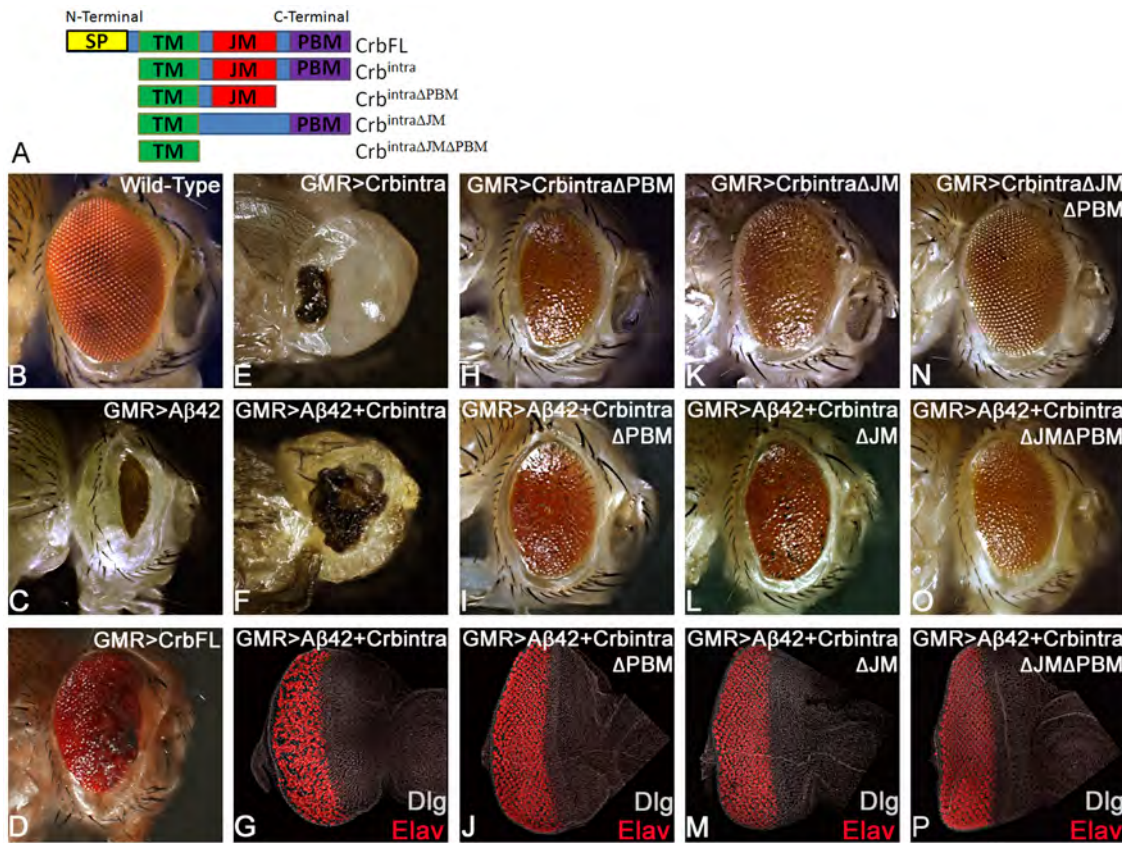


Figure 4. Intracellular domain (ICD) of Crb is required for A β 42 mediated neurodegeneration. (A) A cartoon depicting full length type I transmembrane Crb protein and various truncated constructs used in this study. The full length Crb protein consists of an extracellular domain (ECD), transmembrane domain (TM), and a short cytoplasmic intracellular domain (ICD), which consists of the juxtamembrane Ferm-binding motif (JM) and PDZ-binding motif (PBM) domains [28]. GMR-Gal4 driver was used for the misexpression studies in the differentiating photoreceptor neurons [22]. (B–D) Adult eyes of (B) Wild-Type, (C) GMR>A β 42 (GMR enhancer driving overexpression of human A β 42 in the developing neural retina), and (D) GMR>Crb (FL) are shown as controls. (A, E–F) Misexpression of (E) Crb^{intra} alone, comprising of fully intact ICD, shows a severe phenotype with a small scab on the head cuticle in the adult eye, which is similar to the (F) GMR>A β 42+Crb^{intra} adult eye. (G) In the GMR>A β 42+Crb^{intra} eye disc big gaps and holes between photoreceptors of the ommatidia are seen, Dlg (white) marks the membrane and provide an outline of the imaginal disc and pan neural marker Elav [52] marks the photoreceptors. (A, H–P) In the three other Crb constructs, one of the two domains (JM and PBM) of the ICD is either missing or both of them are missing. (H–J) When Crb is missing either (H–J) PBM, or (K–M) JM, or (N–P) both the PBM and JM domain of the ICD, the GMR>A β 42 neurodegenerative phenotype is restored significantly with the adult eye having a larger size, higher number of ommatidia, and interommatidial bristles. Furthermore, the Elav staining in the eye-imaginal discs shows more organized photoreceptors in comparison to the GMR>A β 42 eye imaginal disc. (H, K, N) The controls (H) GMR>Crb^{intra ΔPBM}, (K) GMR>Crb^{intra ΔJM}, and (N) GMR>Crb^{intra ΔPBM ΔJM} showed adult eye phenotypes that are significantly closer to the wild-type. (I, J) When the PBM domain (GMR>A β 42+Crb^{intra ΔPBM}) is missing, (I) the adult eye and (J) the eye imaginal disc showed significant rescue in comparison to the GMR>A β 42 phenotype. (L, M) When the JM domain (GMR>A β 42+Crb^{intra ΔJM}) is missing, (L) the adult eye and (M) the eye-imaginal disc showed significant rescue in comparison to the GMR>A β 42 phenotype. (O, P) Finally, when both PBM and JM domains of the ICD are missing (GMR>A β 42+Crb^{intra ΔPBM ΔJM}), a significant rescue was seen in (O) the adult eye and (P) the eye imaginal disc in comparison to the GMR>A β 42 phenotype.

doi:10.1371/journal.pone.0078717.g004

Crb^{intra} (Figure 4F, G) showed a neurodegenerative phenotype, it raised the possibility of an additive effect. Further experimentation using the truncated constructs of Crb^{intra} domains disproved this additive effect hypothesis. Targeted misexpression of GMR>A β 42 with Crb^{intra ΔPBM} [28] or Crb^{intra ΔJM} [28] in developing retina resulted in the rescue of the GMR>A β 42 neurodegenerative phenotype as seen in the eye imaginal disc (Figure 4J, M) as well as the adult eye (Figure 4I, L). The controls GMR>Crb^{intra ΔPBM} (Figure 4H) and GMR>Crb^{intra ΔJM} (Figure 4K) exhibit a slightly reduced adult eye. The Crb^{intra} construct lacking both the JM and PBM domains (GMR>Crb^{intra ΔJM ΔPBM} (Figure 4A)) resulted in a near normal adult eye (Figure 4N). Targeted misexpression of GMR>A β 42 with Crb^{intra ΔJM ΔPBM} resulted in the rescue of the GMR>A β 42 neurodegenerative phenotype as seen in the eye imaginal disc

(Fig. 4P), and the adult eye (Fig. 4O). All these results clearly demonstrated that like the full length Crb (Crb FL), the entire ICD (Crb^{intra}) is also responsible for the enhancement of the neurodegenerative phenotype of GMR>A β 42. It suggests that Crb ICD is sufficient enough to carry out the Crb FL function in A β 42 mediated neurodegeneration. When we remove either one or both of the JM and PBM domains from the ICD of Crb, the GMR>A β 42 phenotype is rescued and the ommatidia are restored to near wild-type. This data strongly indicates that both the JM and PBM domains in Crb are essential to suppress the A β 42 effects. There might be a correlative interaction between the JM and PBM domains of Crb in the A β 42 mediated neurodegeneration. However, when we have an intact ICD or full length Crb, there is a severe enhancement of the GMR>A β 42 phenotype. Also, in the loss-of-function *crb* flies

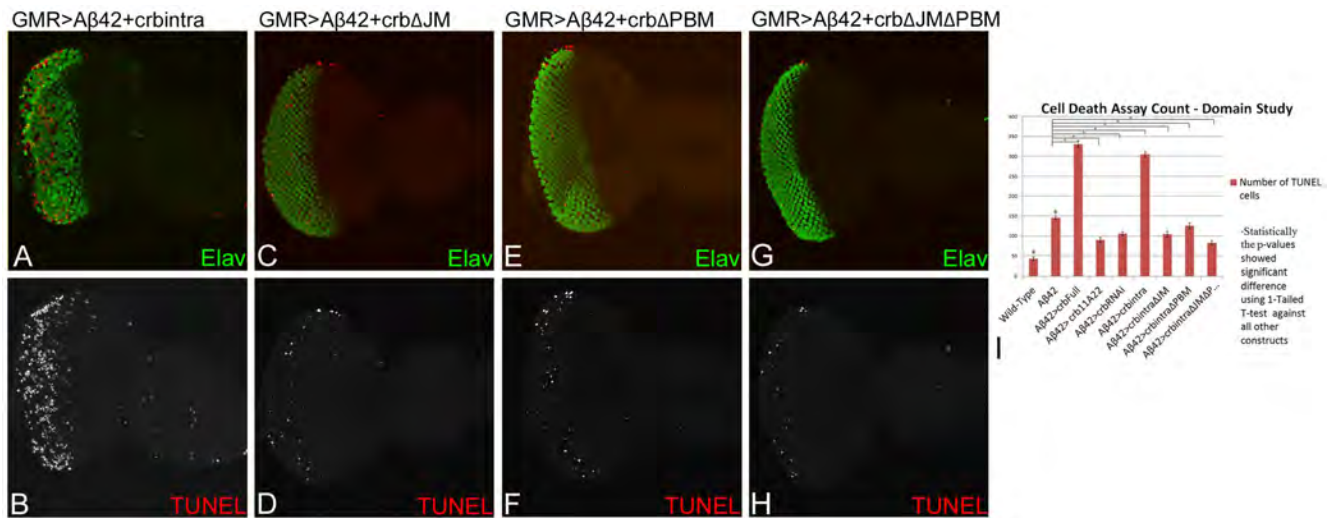


Figure 5. Misexpression of Crb intracellular domain triggers neuronal cell death. (A, C, E, G) The eye-antennal discs are stained with pan neuronal marker Elav (green), marking the photoreceptor neurons, and TUNEL (red), which marks the nuclei of dying cells. (B, D, F, H) The split channels of the TUNEL cells are shown for better depiction of the TUNEL cells alone. (A, B) In the GMR>A β 42+crb^{intra} eye disc, the neurodegenerative phenotype of GMR>A β 42 is enhanced due to increased number of dying photoreceptor neurons as evident from the large number of TUNEL (red) positive cells nuclei, which are (I) calculated quantitatively for all constructs in the bar graph. (A) The dying photoreceptors are clumped and fused together. When we removed either of the PBM, JM or both of these domains within the intracellular domain (ICD) motifs, we see a rescue in the adult eye (Figure 2) and also a (I) decrease in the number of TUNEL positive cells. (C, D) GMR>A β 42+Crb^{intra}ΔJM (when the JM motif is removed) shows an increase in the (C) organization of the photoreceptors within the ommatidia (Elav) and (C, D, I) a decrease in the number of TUNEL positive cells nuclei as compared to the GMR>A β 42+Crb^{intra}. (D) The number of dying cells in GMR>A β 42+Crb^{intra}ΔJM is closer to that seen in the wild-type. A similar result was found (E, F, I) when PBM domain was removed from the ICD motif, GMR>A β 42+Crb^{intra}ΔPBM or (G, H, I) when both the JM and PBM domains were removed from the ICD motif A β 42+Crb^{intra}ΔJMΔPBM. In comparison to GMR>A β 42+Crb^{intra}, we see a significant decrease in the number of TUNEL positive cells in (E, F, I) GMR>A β 42+Crb^{intra}ΔPBM and (G, H, I), A β 42+Crb^{intra}ΔJMΔPBM. (E–H) The number of dying cell nuclei is closer to that seen in the wild-type. Thus, when the ICD is intact (A, B), there is a large number of TUNEL positive cells, which accounts for the adult eye phenotype observed in Figure 2B. However, when either or both of the ICD motifs are removed (C, D, E, F, G, H), there is a significant reduction in the number of TUNEL positive cells as compared to GMR>A β 42+Crb^{intra} and GMR>A β 42.
doi:10.1371/journal.pone.0078717.g005

(GMR>A β 42+crb^{11A22} and GMR>A β 42+crb RNAi) where we see reduced Crb level expression (Figure 1L, O) as compared to the wild-type (Figure 1C), there is a rescue of A β 42 mediated neurodegeneration further validating our hypothesis that Crb levels can modify the neurodegenerative phenotype of A β 42 accumulation. Thus, Crb levels can serve as an excellent biomarker for AD.

To further verify the structure function analysis results, TUNEL assays were performed on all of the constructs. The rationale was to examine if the reduced eye phenotype seen in GMR>A β 42+Crb^{intra} was due to cell death or, on the other hand, if the restored eye as shown by removing either or both of the JM and PBM domains of ICD motifs (Figure 4A) is due to reduced number of TUNEL cells. As mentioned earlier, TUNEL marks the nuclei of dying cells, therefore a reduced number of TUNEL positive cells nuclei corresponds to less cells dying, which will lead to a rescue of GMR>A β 42 neurodegenerative phenotype in the adult eye. We found that the severely reduced adult eye phenotype of GMR>A β 42+Crb^{intra} is in fact due to an increase in the number of TUNEL positive cells as compared to the wild-type and the GMR>A β 42 eye disc (Figure 5A, B, I). The GMR>A β 42+Crb^{intra} exhibits strong neurodegenerative phenotype as evident from disorganized photoreceptor neurons (marked by Elav, green) in the ommatidia. Furthermore, the number of TUNEL positive cells nuclei are increased (Figure 5A, B; red). The TUNEL staining explains the reason for a highly reduced adult eye in GMR>A β 42+Crb^{intra} (Figure 2F). Additionally, when any either JM or PBM or both JM and PBM domains of the ICD motifs were removed in the GMR>A β 42 background, the severity

of neurodegenerative phenotypes was significantly reduced. In GMR>A β 42+Crb^{intra}ΔJM (Figure 5C, D), GMR>A β 42+Crb^{intra}ΔPBM (Figure 5E, F), or GMR>A β 42+Crb^{intra}ΔJMΔPBM (Figure 5G, H), the number of TUNEL positive dying cells nuclei were significantly less than GMR>A β 42 and GMR>A β 42+Crb^{intra} (Figure 5I). All of these results further validate the data shown in Figure 4 and conforms to the adult eye phenotypes of each of these structures.

For all the ICD motifs of Crb, the TUNEL positive cells were counted from five sets of imaginal discs and were used for statistical analysis using Microsoft Excel 2010. The P-values were calculated using one-tailed *t*-test and the error bars represent Standard Deviation from the Mean [3]. All the p-values showed the TUNEL count to be significantly different from GMR>A β 42 and the wild-type (Figure 5I). By studying the domains of Crb with reference to the cell death, we found that misexpression of intact Crb ICD domain in GMR>A β 42 background (GMR>A β 42+Crb^{intra}), resulted in the increased number of TUNEL positive cell (Figure 5I) and was almost six times higher than the wild type eye imaginal disc ($p = 1.5559 \times 10^{-7}$) and nearly two times higher than the GMR>A β 42 eye imaginal disc ($p = 8.7869 \times 10^{-8}$). Removing the JM motif alone (GMR>A β 42+Crb^{intra}ΔJM (Figure 5C, D), PBM motif alone (GMR>A β 42+Crb^{intra}ΔPBM (Figure 5E, F), or by removing both the ICD motifs (GMR>A β 42+Crb^{intra}ΔJMΔPBM (Figure 5G, H) resulted in reduced numbers of TUNEL positive dying cells nuclei. The dying cells nuclei in these truncated constructs (Figure 5C–H) were significantly lower than GMR>A β 42 (for Crb^{intra}ΔJM $p = 3.3329 \times 10^{-5}$, for Crb^{intra}ΔPBM $p = 1.5028 \times 10^{-5}$, for

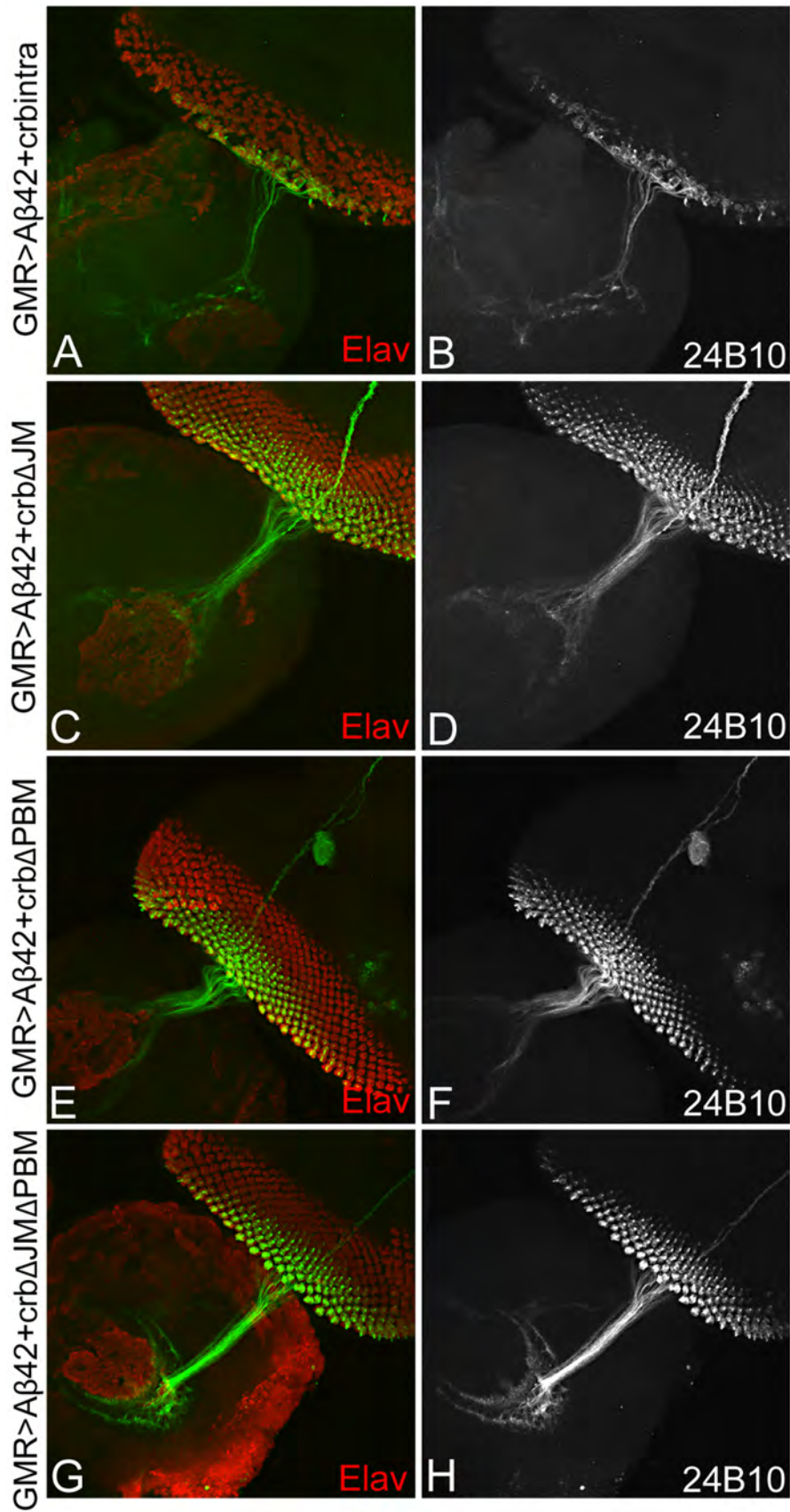


Figure 6. Misexpression of Crb intracellular domain (ICD) can impair axonal targeting. The eye-antennal disc is stained with Elav (red), which marks the photoreceptors, and 24B10 (chaoptin; green), which stains the axons from the retina to the brain [34]. (A, B) Misexpression of intact instar cellular domain ICD $GMR>A\beta 42+Crb^{intra}$ results in clumping of photoreceptors (Elav; A), disorganization of axonal targeting from the retina to the brain as evident from 24B10 staining. (C, D) When the JM motif using $GMR>A\beta 42+Crb^{intra \Delta JM}$, photoreceptor organization as well as the axonal targeting is restored to the wild type. Similarly, removing the (E, F) PBM motif of the ICD using $GMR>A\beta 42+Crb^{intra \Delta PBM}$, or both PBM and JM domain in $GMR>A\beta 42+Crb^{intra \Delta JM \Delta PBM}$, result in restoration of axonal targeting and photoreceptors. Thus, ICD domain of Crb is required for its role in neurodegeneration.
doi:10.1371/journal.pone.0078717.g006

$Crb^{intra \Delta JM \Delta PBM}$ $p = 8.9278 \times 10^{-6}$; Figure 5I). This TUNEL assay further validated our hypothesis that the reduced eye phenotype seen in $GMR>A\beta 42+Crb^{intra}$ (with its fully intact ICD) is primarily due to induction of cell death and the restored eye phenotypes seen when any one or both of the ICD motifs of Crb is/are removed, does indeed have reduced number of dying cells as evident from TUNEL staining.

To further test our hypothesis, we looked at the axonal targeting from the retina to the brain using 24B10 (Chaoptin) in these constructs (Figure 4A). As mentioned earlier, 24B10 shows an organized and orderly axon branching from the retina to the brain in the wild-type background (Figure 3A). However, when we observed the 24B10 staining in the $GMR>A\beta 42+Crb^{intra}$ eye there is extreme disorganization marked by the clumping of axons, as well as Elav (red) positive photoreceptors which results in impairing of axonal targeting from retina to the brain (Figure 6A, B). This data further confirms our TUNEL data using $GMR>A\beta 42+Crb^{intra}$. Additionally, when we analyzed other constructs of Crb by removing either or both of the JM or PBM domains from the ICD motif, there is a rescue of the adult eye (Figure 4A, H–P), a reduction in the number of TUNEL positive (Figure 5C–I), and restoration of the organization of axons from the retina to the brain (Fig. 6 C–H) in all three constructs ($GMR>A\beta 42+Crb^{intra \Delta JM}$ (Figure 6C, D), $GMR>A\beta 42+Crb^{intra \Delta PBM}$ (Figure 6E, F), $GMR>A\beta 42+Crb^{intra \Delta JM \Delta PBM}$ (Figure 6G, H). When the JM motif ($GMR>A\beta 42+Crb^{intra \Delta JM}$ (Figure 6C, D) or the PBM motif ($GMR>A\beta 42+Crb^{intra \Delta PBM}$ (Figure 6E, F) was removed, there is restoration of the axonal targeting as evident from the 24B10 staining and marking the axonal projections innervate the two layers of the brain. Furthermore, when we remove both of the ICD motifs ($GMR>A\beta 42+Crb^{intra \Delta JM \Delta PBM}$ (Figure 6G, H), the axonal connection to the brain is restored to near wild type axonal targeting. These data further validates that the ICD domain of Crb is sufficient enough for Crb function in A β 42 mediated neurodegeneration.

Discussion

Our studies strongly suggest that transmembrane protein Crb is involved in A β 42 mediated neurodegeneration. During wing development, N upregulates *crb* transcription at the dorso-ventral (DV) boundary, and the ability of Crb to inhibit the activity of the γ -secretase complex has been proposed to help refine the N activity domain [43]. Crb functions as a negative regulator of the N signaling pathway [42]. Notch is involved in the development and organization of the dorso-ventral boundary through cell proliferation of the developing eye. Because N and Amyloid Precursor Protein (APP) are cleaved by similar secretases [44] and Crb regulates N, the Crb effects on A β 42 could be caused through N regulation. However, in the $GMR>A\beta 42$ model used in our studies, the A β 42 protein is already cleaved from of APP and does

not require cleavage by β - and γ -secretase. Therefore, our data using the transgenic model suggests that Crb also acts downstream of γ -secretase mediated cleavage of APP. Furthermore, higher levels of Crb can enhance human A β 42 mediated neurodegeneration [3]. Thus, Crb role in modulating A β 42 mediated neurodegeneration is downstream of N signaling pathway.

In addition, Crb is an upstream regulator of the organ size growth control pathway *viz.*, Hippo signaling pathway. Recently, it was shown that Crb interacts with its juxtamembrane FERM-binding motif (JM) with the FERM domain of Expanded (Ex) to regulate growth by affecting the Hippo pathway activity [45–47]. Our structure function analysis studies exhibited that ICD of Crb is sufficient for its role in A β 42 mediated neurodegeneration suggesting that Crb may act independent of its interaction with Hippo pathway member Ex in A β 42 mediated neurodegeneration.

Since Crb ICD is involved in its interaction with apical basal polarity gene localization, there is a strong possibility that higher level of Crb in a $GMR>A\beta 42$ background might affect the apical basal polarity of the retinal photoreceptor neurons which result in neurodegeneration. Mutations in Crb homolog 1 (CRB1) has been shown to cause autosomal recessive retinitis pigmentosa (arRP) and autosomal Leber congenital amaurosis (arLCA) [36]. During *Drosophila* eye development, Crb is required in photoreceptors for stalk elongation [42,48], and in preventing light-dependent retinal degeneration [49]. Mutations in the human Crb homolog (CRB1) result in abnormalities like thick retina and lamination problems [50]. Furthermore, mutant Crb protein is thought to be responsible for retinal degenerations [50]. However, in $GMR>A\beta 42$ background higher levels of Crb protein were responsible for neurodegeneration. Therefore, it is a strong possibility that higher Crb levels may impair apical basal polarity leading to the A β 42 neurodegeneration. Thus, regulating Crb levels can help prevent the onset of neurodegeneration and Crb may serve as one of the biomarker as well as the key therapeutic targets for the AD.

Acknowledgments

Authors thank Bloomington Stock Centre, Developmental Studies Hybridoma Bank (DSHB), Sangchul Nam, Pedro Fernandez-Funez, Justin Kumar, and K. Cho for fly reagents and members of Singh and Kango-Singh Lab for the comments on the manuscript. AMS is a Berry Summer Research Institute Scholar and a member of the undergraduate Honors Program at UD. MT and ORP are supported by the graduate program at the University of Dayton.

Author Contributions

Conceived and designed the experiments: AS MKS. Performed the experiments: AMS RM JN MKS AS ORP. Analyzed the data: AMS MT RM JN. Wrote the paper: AMS MKS AS.

References

- Hardy J (2009) The amyloid hypothesis for Alzheimer's disease: a critical reappraisal. *J Neurochem* 110: 1129–1134.
- O'Brien RJ, Wong PC (2010) Amyloid Precursor Protein Processing and Alzheimer's Disease. *Annu Rev Neurosci*.

3. Tare M, Modi RM, Nainaparampil JJ, Puli OR, Bedi S, et al. (2011) Activation of JNK signaling mediates amyloid-ss-dependent cell death. *PLoS One* 6: e24361.
4. Shankar GM, Li S, Mehta TH, Garcia-Munoz A, Shepardson NE, et al. (2008) Amyloid-beta protein dimers isolated directly from Alzheimer's brains impair synaptic plasticity and memory. *Nat Med* 14: 837–842.
5. Rincon-Limas DE, Jensen K, Fernandez-Funez P (2012) *Drosophila* Models of Proteinopathies: the Little Fly that Could. *Curr Pharm Des*.
6. Pandey UB, Nichols CD (2011) Human disease models in *Drosophila melanogaster* and the role of the fly in therapeutic drug discovery. *Pharmacol Rev* 63: 411–436.
7. Hirth F (2010) *Drosophila melanogaster* in the study of human neurodegeneration. *CNS Neurol Disord Drug Targets* 9: 504–523.
8. Crews L, Masliah E (2010) Molecular mechanisms of neurodegeneration in Alzheimer's disease. *Hum Mol Genet* 19: R12–20.
9. Finelli A, Kelkar A, Song HJ, Yang H, Konsolaki M (2004) A model for studying Alzheimer's A β 42-induced toxicity in *Drosophila melanogaster*. *Mol Cell Neurosci* 26: 365–375.
10. Casas-Tinto S, Zhang Y, Sanchez-Garcia J, Gomez-Velazquez M, Rincon-Limas DE, et al. (2011) The ER stress factor XBP1s prevents amyloid- β neurotoxicity. *Hum Mol Genet* 20: 2144–2160.
11. Moloney A, Sattelle DB, Lomas DA, Crowther DC (2010) Alzheimer's disease: insights from *Drosophila melanogaster* models. *Trends Biochem Sci* 35: 228–235.
12. Iijima-Ando K, Iijima K (2010) Transgenic *Drosophila* models of Alzheimer's disease and tauopathies. *Brain Struct Funct* 214: 245–262.
13. Iijima K, Iijima-Ando K (2008) *Drosophila* models of Alzheimer's amyloidosis: the challenge of dissecting the complex mechanisms of toxicity of amyloid-beta 42. *J Alzheimers Dis* 15: 523–540.
14. Cowan CM, Shepherd D, Mudher A (2010) Insights from *Drosophila* models of Alzheimer's disease. *Biochem Soc Trans* 38: 988–992.
15. Cao W, Song HJ, Gangi T, Kelkar A, Antani I, et al. (2008) Identification of novel genes that modify phenotypes induced by Alzheimer's beta-amyloid overexpression in *Drosophila*. *Genetics* 178: 1457–1471.
16. Bier E (2005) *Drosophila*, the golden bug, emerges as a tool for human genetics. *Nat Rev Genet* 6: 9–23.
17. Kumar JP (2010) Retinal determination the beginning of eye development. *Curr Top Dev Biol* 93: 1–28.
18. Ready DF, Hanson TE, Benzer S (1976) Development of the *Drosophila* retina, a neurocrystalline lattice. *Dev Biol* 53: 217–240.
19. Brachmann CB, Cagan RL (2003) Patterning the fly eye: the role of apoptosis. *Trends Genet* 19: 91–96.
20. Mehlen P, Mille F, Thibert C (2005) Morphogens and cell survival during development. *J Neurobiol* 64: 357–366.
21. Brand AH, Perrimon N (1993) Targeted gene expression as a means of altering cell fates and generating dominant phenotypes. *Development* 118: 401–415.
22. Moses K, Rubin GM (1991) Glass encodes a site-specific DNA-binding protein that is regulated in response to positional signals in the developing *Drosophila* eye. *Genes Dev* 5: 583–593.
23. Tepass U, Theres C, Knust E (1990) crumbs encodes an EGF-like protein expressed on apical membranes of *Drosophila* epithelial cells and required for organization of epithelia. *Cell* 61: 787–799.
24. Campbell K, Knust E, Skaer H (2009) Crumbs stabilises epithelial polarity during tissue remodelling. *J Cell Sci* 122: 2604–2612.
25. Bachmann A, Schneider M, Theilenberg E, Grawe F, Knust E (2001) *Drosophila* Stardust is a partner of Crumbs in the control of epithelial cell polarity. *Nature* 414: 638–643.
26. Bhat MA, Izaddoost S, Lu Y, Cho KO, Choi KW, et al. (1999) Discs Lost, a novel multi-PDZ domain protein, establishes and maintains epithelial polarity. *Cell* 96: 833–845.
27. Bachmann A, Grawe F, Johnson K, Knust E (2008) *Drosophila* Lin-7 is a component of the Crumbs complex in epithelia and photoreceptor cells and prevents light-induced retinal degeneration. *Eur J Cell Biol* 87: 123–136.
28. Klebes A, Knust E (2000) A conserved motif in Crumbs is required for E-cadherin localisation and zonula adherens formation in *Drosophila*. *Curr Biol* 10: 76–85.
29. Singh A, Kango-Singh M, Sun YH (2002) Eye suppression, a novel function of teashirt, requires Wingless signaling. *Development* 129: 4271–4280.
30. League GP, Nam SC (2011) Role of kinesin heavy chain in Crumbs localization along the rhabdomere elongation in *Drosophila* photoreceptor. *PLoS One* 6: e21218.
31. White K, Grether ME, Abrams JM, Young L, Farrell K, et al. (1994) Genetic control of programmed cell death in *Drosophila*. *Science* 264: 677–683.
32. Singh A, Shi X, Choi KW (2006) Lobe and Serrate are required for cell survival during early eye development in *Drosophila*. *Development* 133: 4771–4781.
33. Johnson K, Grawe F, Grzeschik N, Knust E (2002) *Drosophila* crumbs is required to inhibit light-induced photoreceptor degeneration. *Curr Biol* 12: 1675–1680.
34. Zipursky SL, Venkatesh TR, Teplow DB, Benzer S (1984) Neuronal development in the *Drosophila* retina: monoclonal antibodies as molecular probes. *Cell* 36: 15–26.
35. Gunawardena S, Goldstein LS (2001) Disruption of axonal transport and neuronal viability by amyloid precursor protein mutations in *Drosophila*. *Neuron* 32: 389–401.
36. Richard M, Roepman R, Aartsen WM, van Rossum AG, den Hollander AI, et al. (2006) Towards understanding CRUMBS function in retinal dystrophies. *Hum Mol Genet* 15 Spec No 2: R235–243.
37. Garrity PA, Lee CH, Salecker I, Robertson HC, Desai CJ, et al. (1999) Retinal axon target selection in *Drosophila* is regulated by a receptor protein tyrosine phosphatase. *Neuron* 22: 707–717.
38. Laprise P, Beronja S, Silva-Gagliardi NF, Pellikka M, Jensen AM, et al. (2006) The FERM protein Yurt is a negative regulatory component of the Crumbs complex that controls epithelial polarity and apical membrane size. *Dev Cell* 11: 363–374.
39. Nam SC, Choi KW (2003) Interaction of Par-6 and Crumbs complexes is essential for photoreceptor morphogenesis in *Drosophila*. *Development* 130: 4363–4372.
40. Sotillos S, Diaz-Meco MT, Caminero E, Moscat J, Campuzano S (2004) DaPKC-dependent phosphorylation of Crumbs is required for epithelial cell polarity in *Drosophila*. *J Cell Biol* 166: 549–557.
41. Morishima Y, Gotoh Y, Zieg J, Barrett T, Takano H, et al. (2001) Beta-amyloid induces neuronal apoptosis via a mechanism that involves the c-Jun N-terminal kinase pathway and the induction of Fas ligand. *J Neurosci* 21: 7551–7560.
42. Richardson EC, Pichaud F (2010) Crumbs is required to achieve proper organ size control during *Drosophila* head development. *Development* 137: 641–650.
43. Herranz H, Stamatakis E, Feiguin F, Milan M (2006) Self-refinement of Notch activity through the transmembrane protein Crumbs: modulation of gamma-secretase activity. *EMBO Rep* 7: 297–302.
44. Kimberly WT, Esler WP, Ye W, Ostaszewski BL, Gao J, et al. (2003) Notch and the amyloid precursor protein are cleaved by similar gamma-secretase(s). *Biochemistry* 42: 137–144.
45. Chen CL, Gajewski KM, Hamaratoglu F, Bossuyt W, Sansores-Garcia L, et al. (2010) The apical-basal cell polarity determinant Crumbs regulates Hippo signaling in *Drosophila*. *Proc Natl Acad Sci U S A* 107: 15810–15815.
46. Ling C, Zheng Y, Yin F, Yu J, Huang J, et al. (2010) The apical transmembrane protein Crumbs functions as a tumor suppressor that regulates Hippo signaling by binding to Expanded. *Proc Natl Acad Sci U S A* 107: 10532–10537.
47. Robinson BS, Huang J, Hong Y, Moberg KH (2010) Crumbs regulates Salvador/Warts/Hippo signaling in *Drosophila* via the FERM-domain protein Expanded. *Curr Biol* 20: 582–590.
48. Richard M, Muschalik N, Grawe F, Ozuyaman S, Knust E (2009) A role for the extracellular domain of Crumbs in morphogenesis of *Drosophila* photoreceptor cells. *Eur J Cell Biol* 88: 765–777.
49. Bulgakova NA, Knust E (2009) The Crumbs complex: from epithelial-cell polarity to retinal degeneration. *J Cell Sci* 122: 2587–2596.
50. Jacobson SG, Cideciyan AV, Aleman TS, Pianta MJ, Sumaroka A, et al. (2003) Crumbs homolog 1 (CRB1) mutations result in a thick human retina with abnormal lamination. *Hum Mol Genet* 12: 1073–1078.
51. Tepass U (1996) Crumbs, a component of the apical membrane, is required for zonula adherens formation in primary epithelia of *Drosophila*. *Dev Biol* 177: 217–225.
52. Dhanasekaran DN, Reddy EP (2008) JNK signaling in apoptosis. *Oncogene* 27: 6245–6251.